HYDROLOGICAL PROCESSES
Hydrol. Process. **31**, 69–89 (2017)
Published online 10 October 2016 in Wiley Online Library
(wileyonlinelibrary.com) DOI: 10.1002/hyp.10965

Frequency analysis of nonstationary annual maximum flood series using the time-varying two-component mixture distributions

Lei Yan,[1] Lihua Xiong,[1]* Dedi Liu,[1] Tiesong Hu[1] and Chong-Yu Xu[1,2]

[1] *State Key Laboratory of Water Resources and Hydropower Engineering Science, Wuhan University, Wuhan 430072, China*
[2] *Department of Geosciences, University of Oslo, PO Box 1022 Blindern, N-0315 Oslo, Norway*

Abstract:

The most popular practice for analysing nonstationarity of flood series is to use a fixed single-type probability distribution incorporated with the time-varying moments. However, the type of probability distribution could be both complex because of distinct flood populations and time-varying under changing environments. To allow the investigation of this complex nature, the time-varying two-component mixture distributions (TTMD) method is proposed in this study by considering the time variations of not only the moments of its component distributions but also the weighting coefficients. Having identified the existence of mixed flood populations based on circular statistics, the proposed TTMD was applied to model the annual maximum flood series of two stations in the Weihe River basin, with the model parameters calibrated by the meta-heuristic maximum likelihood method. The performance of TTMD was evaluated by different diagnostic plots and indexes and compared with stationary single-type distributions, stationary mixture distributions and time-varying single-type distributions. The results highlighted the advantages of TTMD with physically-based covariates for both stations. Besides, the optimal TTMD models were considered to be capable of settling the issue of nonstationarity and capturing the mixed flood populations satisfactorily. Copyright © 2016 John Wiley & Sons, Ltd.

KEY WORDS flood frequency analysis; nonstationarity; time-varying two-component mixture distributions (TTMD); time-varying moments; circular statistics; the Weihe River

Received 20 December 2015; Accepted 17 July 2016

INTRODUCTION

As pointed out by the Scientific Decade 2013–2022 of IAHS, entitled 'Panta Rhei – Everything Flows' (Montanari *et al*., 2013), global climate and hydrological system are suffering substantial changes under changing environments. To improve the understanding and interpretation of changing properties of hydrological system, nonstationary hydrological frequency analysis methods have been recommended to be essential under the assertion that 'stationarity is dead' (Milly *et al*., 2015; Milly *et al*., 2008). However, this assertion is questioned by several thoughtful papers holding the opposite viewpoint in recent years (Koutsoyiannis and Montanari, 2014; Matalas, 2012; Montanari and Koutsoyiannis, 2014; Serinaldi and Kilsby, 2015). The academic debate about whether stationarity is dead focuses on the definition and interpretation of the scientific concept of stationarity and the reliability of the nonstationary models to make future predictions. In spite of these hot debates, one point has been shared that the assumption of stationarity, a conservative but reliable strategy in the practical engineering (Koutsoyiannis and Montanari, 2014; Lins and Cohn, 2011; Prosdocimi *et al*., 2015), may be invalid in nonstationary situations (López and Francés, 2013; Read and Vogel, 2015; Salas and Obeysekera, 2013; Villarini *et al*., 2009a; Xiong *et al*., 2015a; Xiong *et al*., 2015b). Therefore, it is necessary to perform nonstationary frequency analysis to investigate the changes in hydrological system, with the ultimate goal to support future water resources management strategies and hydraulic engineering design (Villarini *et al*., 2015; Read and Vogel, 2015; Sarhadi *et al*., 2016).

In the nonstationary hydrological frequency analysis, the most popular practice is to assume that the type of probability distributions is of the simple single form and is also invariant while the statistical parameters or moments are assumed to be changing with time or physical covariates (Lima *et al*., 2015; Liu *et al*., 2015; Condon *et al*., 2015; Vogel *et al*., 2011; Strupczewski

*Correspondence to: Lihua Xiong, State Key Laboratory of Water Resources and Hydropower Engineering Science, Wuhan University, Wuhan 430072, China.
E-mail: xionglh@whu.edu.cn

et al., 2001). The ever employed single-type distributions include the two-parameter distributions, i.e. Gumbel, Weibull, Gamma and Lognormal (Du *et al*., 2015; Giraldo Osorio and García Galiano, 2012; Jiang *et al*., 2015; Li and Tan, 2015; Villarini *et al*., 2009a; Villarini *et al*., 2009b), and three-parameter distributions, i.e. general extreme value (GEV) (Cannon, 2010; El Adlouni *et al.*, 2007) and Pearson type III (Strupczewski *et al*., 2001; Xiong *et al*., 2014).

The heterogeneity of annual maximum flood series (AMFS) due to climate change and different flood-generating mechanisms would lead to the changes not only in statistical parameters but also in the type of probability distributions (Franks and Kuczera, 2002; Singh *et al*., 2005; Villarini and Smith, 2010). Studies have demonstrated the existence of flood records arising from several distinct populations due to many factors such as different types of flood-generating mechanisms (e.g. thunderstorms, typhoon, tropical cyclone and snowmelt), changes in land-cover types and basin properties (channel characteristics and soil moisture contents) and suggested mixture distribution in frequency analysis (Villarini, 2016; Smith *et al*., 2011; Singh *et al*., 2005; Alila and Mtiraoui, 2002; Rossi *et al*., 1984; Woo and Waylen, 1984).

As emphasized by Klemeš (1986, 1994, 2000), Alila and Mtiraoui (2002) and Villarini and Smith (2010), before conducting mixture distribution modelling, scientific evidence of mixed populations should be provided to strengthen the process understanding or physical understanding of mixture nature of flooding, rather than conducting a statistical exercise without much attention given to the physical process of flooding. If long-term meteorological information and geomorphological data are available, it is feasible to examine mixed flood populations through analysis of distinct climate mechanisms (e.g. different storm types and El Niño-Southern Oscillation conditions) and basin properties (channel characteristics and soil moisture contents). Whereas in cases without such data, mixed populations or corresponding flood-generating mechanisms can be characterized through the analysis of seasonality (Rossi *et al*., 1984; Sivapalan *et al*., 2005; Villarini and Smith, 2010), based on various approaches such as the widely used circular or directional statistics method (Black and Werritty, 1997; Cunderlik *et al*., 2004; Chen *et al*., 2010; Chen *et al*., 2013; Köplin *et al*., 2014; Dhakal *et al*., 2015; Villarini, 2016).

Once the existence of mixed flood populations is identified, it is appropriate and reasonable to turn to mixture distribution modelling. To solve the problem of mixed flood populations, two classes of statistical inference methods have been proposed for hydrological applications, i.e. the stationary mixture distributions for the AMFS (no prior separation of the flood processes and classification of the observations) (Alila and Mtiraoui, 2002; Singh and Sinclair, 1972; Grego and Yates, 2010) and probability distributions for seasonal maximum series (requiring a prior separation of the flood processes and classification of the observations) (Strupczewski *et al*., 2012; US Water Resources Council (USWRC), 1981; Waylen and Woo, 1982). However, in practice, because of the complexities of flood-generating mechanisms and the lack of long-term meteorological data needed for the classification of flood records, a prior separation of the flood processes may not always be feasible for deriving probability distributions for seasonal maximum series. Thus, the stationary mixture distributions for AMFS, which do not require a prior separation of the flood processes, have been widely applied in flood frequency analysis with several standard component distributions (e.g. Lognormal, Gamma, Weibull, Gumbel, GEV and Log Pearson type III) (Alila and Mtiraoui, 2002; Evin *et al*., 2011; Rossi *et al*., 1984; Stedinger *et al*., 1993; Villarini *et al*., 2011). Compared with the stationary single-type distributions, the stationary mixture distributions are able to better model different types of skewness and tail behaviour through an appropriate selection of their components (Alila and Mtiraoui, 2002; McLachlan and Peel, 2000; Rossi *et al*., 1984).

However, stationary mixture distributions are still inadequate to solve the problem that either statistical parameters or distribution types are prone to change in the nonstationary situations. To our knowledge, there have been very few studies investigating the variations in distribution types in the nonstationary situations. Zeng *et al.* (2014) studied the nonstationarity of AMFS in perspective of abrupt change using change point detection and mixture distributions, rather than in perspective of temporal variation of component distributions' parameters. The stationary mixture distributions of Pearson type III were employed to fit the two sub-series of AMFS, divided by the change point detected prior, and the results indicated that stationary mixture distributions considering change point performed much better than stationary single-type distributions in modelling the whole nonstationary flood series. In the study of annual streamflow and spring flood peaks, Evin *et al.* (2011) investigated the two-component mixture distributions for a nonstationary process by introducing a time-varying weighting coefficients via the Bayesian approach, with the parameters of component distributions (Normal, Gamma and Gumbel) assumed to be invariant. In the aforementioned two examples, the parameters of the component distributions were assumed to be invariant within a given time period, which may still not be flexible for applying the mixture distributions in the nonstationary hydrological frequency analysis. Khaliq *et al.* (2006) suggested a nonstationary modelling of flood

data be performed using the mixture distributions with either linear or non-linear trends assumed for the parameters of the component distributions.

To accommodate all possible scenarios in the nonstationary flood frequency analysis, i.e. not only the statistical parameters but also the type of probability distributions could be changing, this study extends the stationary two-component mixture distributions into the time-varying two-component mixture distributions (TTMD). For TTMD, both the parameters of individual component distribution and the weighting coefficients could be time-varying. Three different combinations of component distributions for TTMD were considered, i.e. mixture of Lognormal and Weibull, mixture of Gamma and Lognormal and mixture of Gamma and Weibull. Either time or physical covariates, i.e. irrigation area (*ia*) and precipitation (*prec*), were employed as explanatory variables to model the evolution of time-varying component distributions' parameters and the time-varying weighting coefficients. To estimate the larger number of parameters of the TTMD model, a meta-heuristic maximum likelihood (MHML) parameter estimation approach, incorporating simulated annealing algorithm (SAA) and maximum likelihood estimation (MLE), was also proposed. As case studies, the proposed TTMD method was applied to two stations in the Weihe River basin (WRB), and its performance was compared with the stationary single-type distributions, the stationary mixture distributions and the time-varying single-type distributions.

This paper is organized as follows. First, the methodology used in the paper is presented. Second, we describe the study area and the data used in this study. Third, the applications and results of the TTMD model are demonstrated. Finally, the conclusions along with some discussions are drawn.

METHODOLOGY

The methodologies used in the paper include the seasonality analysis of AMFS based on circular statistics, nonstationary frequency analysis using the single-type distributions, the method of stationary two-component mixture distributions, TTMD, time-varying moments method to describe variation of component distributions' parameters and weighting coefficients, the parameter estimation method, and the model selection criterion and the goodness-of-fit test.

Examination of mixed populations based on detection of seasonality of AMFS

Analyses of flood seasonality have been widely applied to characterize different flood-generating mechanisms (Rossi *et al*., 1984; De Michele and Rosso, 2002; Sivapalan *et al*., 2005; Villarini and Smith, 2010; Smith *et al*., 2011; Villarini, 2016). Thus, mixed flood populations are examined via the use of seasonality as a substitute for distinct flood-generating mechanisms in this study. The seasonality analysis is based on circular statistics, whose flow chart is shown in Figure 1.

The date of occurrence of flood events within a year, denoted by D, can be described as polar coordinates θ on the circumference of a unit circle by the circular statistics method. For the annual maximum flood event y of year t, its occurrence date is denoted by D_{y_t} and can be converted to an angular observation on the unit circle using

$$\theta_{y_t} = D_{y_t}\frac{2\pi}{L} \quad 0 \le \theta_{y_t} \le 2\pi \tag{1}$$

where L is the length of a year ($L = 365$ or $L = 366$ for a leap year) and θ_{y_t} is the angular observation (in radians) of the flood event y_t.

The mean direction of the sample of m flood events' dates, denoted by the polar coordinate $\overline{\theta}$, can then be obtained by

$$\overline{a} = \frac{1}{m}\sum_{t=1}^{m}\cos\left(\theta_{y_t}\right) \tag{2}$$

$$\overline{b} = \frac{1}{m}\sum_{t=1}^{m}\sin\left(\theta_{y_t}\right) \tag{3}$$

$$\overline{\theta} = \arctan\left(\frac{\overline{b}}{\overline{a}}\right) \tag{4}$$

The variability of occurrences of m flood events can be calculated using the sample mean resultant length (Burn, 1997), given by

$$\overline{r} = \sqrt{\overline{a}^2 + \overline{b}^2} \quad 0 \le \overline{r} \le 1 \tag{5}$$

$\overline{r}$ is a measure of the spread of the data, ranging from 0 to 1. Values closer to 0 indicate greater variability in the date of occurrence of flood events, while values closer to 1 indicate almost all the flood events that occur on the same date.

Three different models are used to fit circular data, i.e. uniform model, reflective symmetric model and asymmetric model. From the perspective of statistical inference, firstly, it is fundamental to test whether or not the circular data are uniformly distributed. In cases where we cannot reject the null hypothesis of circular uniformity, there would be no need to employ more complicated models (Pewsey *et al*., 2013; Villarini, 2016). In this study, the Rayleigh test and some widely used omnibus tests (Kuiper, Watson and Rao spacing tests) are applied to test for unimodal and other types of departure from uniformity. For detailed information about these tests, see Mardia and Jupp (2000).

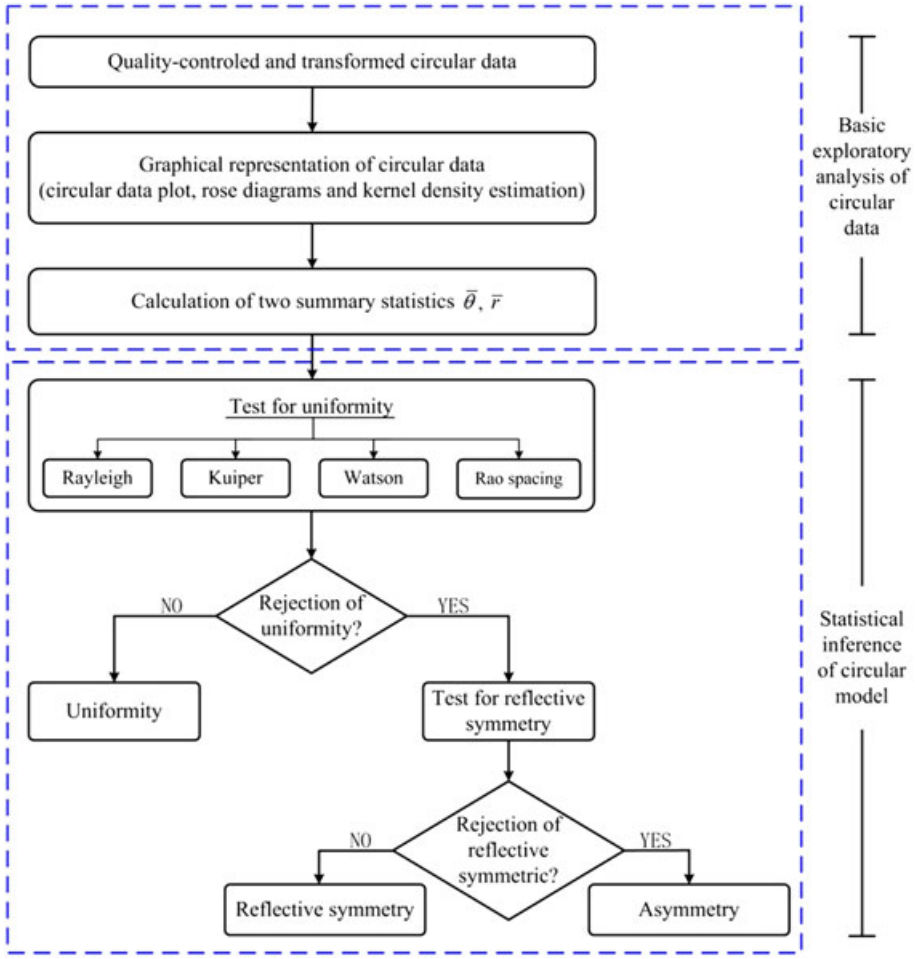

Figure 1. Schematic diagram of exploratory analysis of circular data and statistical inference of circular model

If the null hypothesis of uniformity is rejected, we need to go further with the test for more complicated models (reflective symmetric and asymmetric model). There are two versions of the test for reflective symmetric, depending on the sample size m. If the sample size is larger than 50 ($m > 50$), the asymptotic theory-based test is used, whereas the bootstrap version of test is recommended for smaller sample size ($m < 50$) (Pewsey *et al*., 2013).

If the null hypothesis of reflective symmetry can also be rejected, the seasonality is identified as asymmetry, including multimodal models (i.e. finite mixtures of unimodal symmetric and asymmetric models) (Villarini, 2016). Therefore, in cases in which the asymmetric model is examined, the flood series can be considered as results of distinct flood-generating mechanisms or mixed populations.

Nonstationary frequency analysis using single-type distribution

In the current study, for comparative purpose with the proposed TTMD model, firstly, the stationary single-type distributions and time-varying single-type distributions were constructed to model the AMFS using time-varying moments method built in the framework of generalized addictive models in location, scale and shape (Rigby and Stasinopoulos, 2005), which have been a popular practice in the nonstationary frequency analysis of hydrological series (Jiang *et al*., 2015; Xiong *et al*., 2014; Galiatsatou *et al*., 2016; Zhang *et al*., 2014; Villarini *et al*., 2009a, 2010). In the implementation of the generalized addictive models in location, scale and shape model, statistical parameters of the selected distributions were expressed as a linear or non-linear function of the time or physically-based variables, i.e. irrigation area (*ia*) and precipitation (*prec*).

Based on the four types of popular flood frequency distributions categorized by Malamud and Turcotte (2006) and El Adlouni *et al.* (2008), i.e. the Normal family (e.g. Normal, Lognormal and Lognormal type III), the GEV family (e.g. GEV, Gumbel and Weibull), the Pearson type III family (e.g. Gamma, Pearson type III and Log Pearson type III) and the generalized Pareto distribution, Lognormal, Weibull and Gamma were

selected (Table I). In the application of the time-varying single-type distribution, four scenarios were developed: (1) both the location and scale parameters are constant, i.e. stationary single-type distribution treated as benchmark for comparison; (2) the location parameter is time-varying while the scale parameter is constant; (3) the location parameter is constant, while the scale parameter is time-varying and (4) both the location and scale parameters are time-varying. The optimal model for each covariate and distribution was selected by Akaike information criterion (AIC) (Akaike, 1974) and Schwarz Bayesian criterion (SBC) (Schwarz, 1978).

Stationary two-component mixture distributions

In the field of hydrology, the concept of mixture distributions was first proposed by Singh and Sinclair (1972) to address the issue of mixed populations in the flood frequency analysis and has been widely accepted and applied by researchers around the world. For the sake of completeness, the basic definitions and mathematical interpretations of the mixture distributions are briefly described as follows. Observations of AMFS at time t are denoted by y_t, and the corresponding probability density function of $y_t(t=1,2,\ldots,m)$ is denoted by $f(y_t|\boldsymbol{\theta},\boldsymbol{w})$, which is given by

$$f(y_t|\boldsymbol{\theta},\boldsymbol{w}) = \sum_{i=1}^{k} w_i f_i(y_t|\boldsymbol{\theta}_i) \tag{6}$$

$$\sum_{i=1}^{k} w_i = 1 \tag{7}$$

in which $f_i(y_t|\boldsymbol{\theta}_i)$ is the ith density component of mixture distributions with the vector of parameters set $\boldsymbol{\theta}_i$. w_i is a weighting coefficient ($0 \le w_i \le 1$) denoting the probability of y_t belonging to the ith density component. $\boldsymbol{\theta}=\{\boldsymbol{\theta}_1, \ldots, \boldsymbol{\theta}_k\}$ and $\boldsymbol{w}=(w_1,\ldots,w_k)$. k is the number of mixture components.

As pointed out by Alila and Mtiraoui (2002), the number of mixture components should be kept to a minimum in the applications of Equations 6 and 7, for the reason that the increase in the number of mixture components requires larger number of observations and tends to make the method of parameter estimation less robust and less accurate, especially for the case of TTMD, which has more parameters. Therefore, in this study, the two-component mixture distributions method was employed to reduce the complexities of parameter estimation, with the probability density function given by

$$f(y_t|\boldsymbol{\theta},w) = wf_1(y_t|\boldsymbol{\theta}_1) + (1-w)f_2(y_t|\boldsymbol{\theta}_2) \tag{8}$$

where w and $1-w$ denote the probability of y_t belonging to populations 1 and 2, respectively, and vector of parameters set $\boldsymbol{\theta}=\{\boldsymbol{\theta}_1,\boldsymbol{\theta}_2\}$ represents the distribution parameters related to each component distribution.

A large proportion of studies engaged in mixture of continuous distributions have focused on mixture of Gaussian distributions. However, symmetric distributions are improper to model flood data, which are generally highly skewed or kurtotic. Although log transformation can be applied to flood data, the results (AIC and SBC) calculated based on log-transformed data would not be comparable with those based on original data and extreme distributions. Thus, mixture of Gaussian distributions is not considered in this study. In keeping with the modelling of time-varying single-type distributions, three two-parameter distributions, i.e. Lognormal (LN), Weibull (WEI) and Gamma (GA), were considered as component distributions to build the mixture distributions in this study.

Table I. Summary of the three two-parameter distributions composing the two-component mixture distributions used to model the flood series in this study.

Distributions	Probability density function	Distribution moments	Link functions
Lognormal	$f_Z(z\|\mu,\sigma) = \frac{1}{\sqrt{2\pi}\sigma}\frac{1}{z}\exp\left\{-\frac{[\log(z)-\mu]^2}{2\sigma^2}\right\}$ $z>0, \mu>0, \sigma>0$	$E(Z)=\omega^{1/2}e^{\mu}$ $Var(Z)=\omega(\omega-1)e^{2\mu}$ $\omega=\exp(\sigma^2)$	$h(\mu)=\mu$ $h(\sigma)=\ln(\sigma)$
Gamma	$f_Z(z\|\mu,\sigma) = \frac{1}{(\mu\sigma^2)^{1/\sigma^2}}\frac{z^{\left(1/\sigma^2-1\right)}e^{-z/\left(\mu\sigma^2\right)}}{\Gamma(1/\sigma^2)}$ $z>0, \mu>0, \sigma>0$	$E(Z)=\mu$ $\mathrm{Var}(Z)=\mu^2\sigma^2$	$h(\mu)=\ln(\mu)$ $h(\sigma)=\ln(\sigma)$
Weibull	$f_Z(z\|\mu,\sigma) = \frac{\sigma z^{\sigma-1}}{\mu^{\sigma}}\exp\left[-\left(\frac{z}{\mu}\right)^{\sigma}\right]$ $z>0, \mu>0, \sigma>0$	$E(Z)=\mu\Gamma\left(\frac{1}{\sigma}+1\right)$ $\mathrm{Var}(Z)=\mu^2\left\{\Gamma\left(\frac{2}{\sigma}+1\right)-\left[\Gamma\left(\frac{1}{\sigma}+1\right)\right]^2\right\}$	$h(\mu)=\ln(\mu)$ $h(\sigma)=\ln(\sigma)$

Time-varying two-component mixture distributions

For TTMD, both the parameters of individual component distribution and the weighting coefficients could be time-varying. Thus, TTMD is expressed as

$$f\left(y_t|\boldsymbol{\theta}^t, w^t\right) = w^t f_1\left(y_t|\boldsymbol{\theta}_1^t\right) + (1-w^t) f_2\left(y_t|\boldsymbol{\theta}_2^t\right) \quad (9)$$

where $\boldsymbol{\theta}^t = \left\{\boldsymbol{\theta}_1^t, \boldsymbol{\theta}_2^t\right\}$ represent the time-varying component distributions' parameters of $f_1(\cdot)$ and $f_2(\cdot)$, respectively, and w^t is the time-varying weighting coefficient and should be in the interval of $[0, 1]$. Correspondingly, the cumulative probability of the TTMD is given by

$$F\left(y_t|\boldsymbol{\theta}^t, w^t\right) = w^t F_1\left(y_t|\boldsymbol{\theta}_1^t\right) + (1-w^t) F_2\left(y_t|\boldsymbol{\theta}_2^t\right) \quad (10)$$

On the basis of Equation 9, eight scenarios are generated for the TTMD models (Figure 2), considering the combination of different variation types of component distributions' parameters and the weighting coefficients.

Time variation in the parameters of component distributions and weighting coefficients

For the time-varying moments of two-parameter component distributions $f_i\left(y_t|\mu_i^t, \sigma_i^t\right)$ $(i=1,2)$, both the location parameter μ_i^t and scale parameter σ_i^t can be expressed as a linear or non-linear function of the explanatory variables x_j^t $(j=1,2,\ldots,n)$ through the monotonic link functions given by

$$\begin{aligned} h\left(\mu_i^t\right) &= \alpha_{i0} + \sum_{j=1}^{n} \alpha_{ij} x_j^t \\ h\left(\sigma_i^t\right) &= \beta_{i0} + \sum_{j=1}^{n} \beta_{ij} x_j^t \end{aligned} \quad (11)$$

where $h(\cdot)$ denotes the link function of each statistical parameter, $\boldsymbol{\alpha} = (\alpha_{10}, \ldots, \alpha_{1n}, \alpha_{20}, \ldots, \alpha_{2n})^{\mathrm{T}}$, and $\boldsymbol{\beta} = (\beta_{10}, \ldots, \beta_{1n}, \beta_{20}, \ldots, \beta_{2n})^{\mathrm{T}}$ represent the parameters for describing μ_i^t and σ_i^t, respectively.

Similar to the time-varying parameters of component distributions, the time-varying weighting coefficient w^t can also be expressed as a function of explanatory variables x_j^t $(j=1,2,\ldots,n)$. It should be noted that the value of w^t must be kept in the interval of $[0, 1]$; thus, the expression of w^t is written as

$$w^t = \frac{1}{1 + \exp\left(\varepsilon_0 + \sum_{j=1}^{n} \varepsilon_j x_j^t\right)} \quad (12)$$

where $\boldsymbol{\varepsilon} = (\varepsilon_0, \varepsilon_1, \ldots, \varepsilon_n)^{\mathrm{T}}$ denotes the parameters for describing w^t.

The determination of explanatory variables (or covariates) is an important procedure in constructing TTMD. In this study, both time and physically-based variables (i.e. *ia* and *prec*) were introduced as covariates to model the evolution trends of component distributions' parameters and weighting coefficients.

Parameter estimation

The parameters of TTMD in Equation 9 need to be estimated jointly from the AMFS. Many parameter estimation approaches have been proposed to estimate the statistical parameters of mixture distributions (Evin *et al*., 2011; Fiorentino *et al*., 1987; Leytham, 1984; Rossi *et al*., 1984). Among them, the expectation–maximization (EM) algorithm is the most popular approach despite its weakness of local maximization and divergence with small samples. With the development of Markov chain Monte Carlo method, Bayesian approach is now feasible

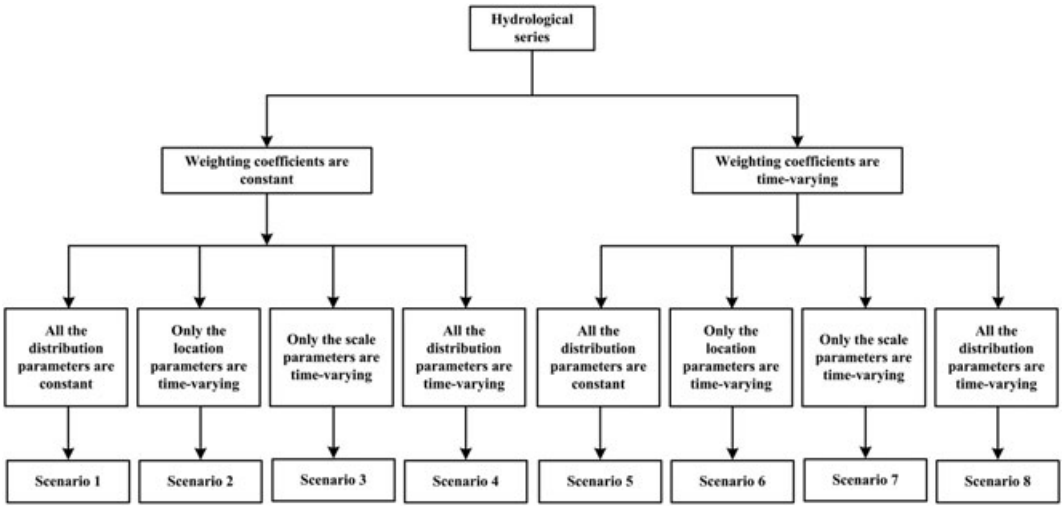

Figure 2. Scenarios generated for the TTMD models. (Scenario 1 represents the stationary mixture model served as a comparison benchmark)

and has been an alternative of EM. However, Bayesian approach requires proper assumption of prior distribution and generally requires long computation time (McLachlan and Peel, 2000). In recent years, meta-heuristic optimization algorithms (e.g. genetic algorithm and SAA) have achieved more and more applications in the parameter estimation of mixture distributions (Lee and Jeong, 2014; Zeng *et al*., 2014; Hassanzadeh *et al*., 2011). Shin *et al.* (2014) proposed a parameter estimation method by incorporating meta-heuristic and MLE, abbreviated by MHML, and found the superiority of MHML method compared with the EM algorithm. The MHML estimation approach has advantages in finding global maximum and can be flexibly applied to various mixture distributions.

For the given observed flood series $y_t (t = 1, 2, \ldots, m)$, the log-likelihood function for the TTMD is expressed by

$$\begin{aligned} l &= \ln L \\ &= \ln \prod_{t=1}^{m} f(y_t | \boldsymbol{\theta}^t, w^t) \\ &= \sum_{t=1}^{m} \ln \left\{ w^t f_1 \left(y_t | \boldsymbol{\theta}_1^t \right) + (1 - w^t) f_2 \left(y_t | \boldsymbol{\theta}_2^t \right) \right\} \end{aligned} \tag{13}$$

To maximize the log-likelihood function in Equation 13, the conventional Newton–Raphson method does not work because of complicated information matrix and local optimum problem. To overcome these deficiencies, a meta-heuristic algorithm named SAA (Kirkpatrick *et al*., 1983; Černý, 1985) was employed.

Simulated annealing algorithm emulates the gradual cooling process (i.e. annealing) of material, during which the temperature decreases stepwise. At each temperature, an initial configuration is generated and used to evaluate the corresponding objective function E_a (energy value). Then a small displacement is imposed on current configuration to calculate a new objective function E_b. If $\delta E = E_b - E_a < 0$, this new configuration is accepted as the best. Otherwise, it is accepted with the probability

$$p(\delta E) = exp\left(-\frac{\delta E}{KT} \right) \tag{14}$$

in which K is the Boltzmann's constant and T is the current temperature. If this probability is higher than a random number, this configuration is accepted as the best, although it is not better than the previous solution. Once the system has reached equilibrium at the current temperature T, the algorithm continues and reduces temperature gradually until the system reaches its minimum temperature (Dowsland and Thompson, 2012; Kirkpatrick *et al*., 1983; Černý, 1985).

In this study, the optimization problem in SAA is a constrained single-objective optimization with minimizing the opposite of the log-likelihood function l in Equation 13, i.e. $-l$. The main procedures of the SAA-based MHML for the TTMD are summarized as follows:

1. Initialize the temperature T_0.
2. Set a variation range for the parameters of TTMD and generate initial solution configuration randomly.
3. Calculate the value of objective function E_a (i.e. $-l_a$).
4. Generate a new solution configuration by imposing a small displacement on current configuration and calculate the value of objective function E_b (i.e. $-l_b$).
5. If $\delta E = E_b - E_a = l_a - l_b < 0$, the new solution is accepted. Otherwise, accept the new solution with a probability $p(\delta E)$.
6. Repeat steps 4 and 5 at current temperature.
7. Reduce the temperature and repeat steps 2–6 until the stop criterion is met.

Model selection criterion and goodness-of-fit test

In this study, a series of TTMD models were built considering different combinations and variation types of parameters. To avoid model overfitting and determine the optimal TTMD model for nonstationary flood frequency analysis, the AIC (Akaike, 1974) was employed, which is given by

$$\mathrm{AIC} = -2 l_{\max} + 2p \tag{15}$$

where $l_{\max}$ is the maximized value of the log-likelihood function 13 for each candidate TTMD model and p is the total number of independently adjusted parameters of the model. In addition to AIC, the SBC (Schwarz, 1978) or Bayesian information criterion was also used to select the optimal model, which is given by

$$\mathrm{SBC} = -2 l_{\max} + \ln(m) p \tag{16}$$

in which m is the number of observations of the AMFS. It should be noted that the penalty term (the second term in Equations 15 and 16) introduced by SBC is larger than that of AIC in handling the problem of overfitting of TTMD models. The models with lower AIC and SBC scores are considered to be better ones.

The goodness-of-fit of the established TTMD models is evaluated by the Q-Q plot, the worm plot (or detrended Q-Q plot) (van Buuren and Fredriks, 2001) and the centiles curve plot. Q-Q plot is a popular diagnostic technique in the stationary situations and is also applicable for nonstationary situations. The normalized quantiles residuals are denoted by $r_t = \Phi^{-1}(u_t)$, where $\Phi^{-1}(\cdot)$ is the inverse cumulative density function of a standard normal distribution and u_t is the cumulative probability and in this study is given by $u_t = F(y_t | \boldsymbol{\theta}^t, w^t)$. The empirical quantiles are calculated by $v_t = \Phi^{-1}(p_t)$, where $p_t = \frac{r(y_t) - 0.5}{m}$ is the Hazen's formula for plotting

empirical points and $r(y_t)$ is the rank order of the observations y_t $(t = 1, 2, \ldots, m)$. The more closely the Q-Q plot locates along the 1 : 1 line, the better the fitting qualities of the distribution are. Additionally, the fitted time series (quantiles calculated by substituting empirical frequency of the observations, p_t, into the established

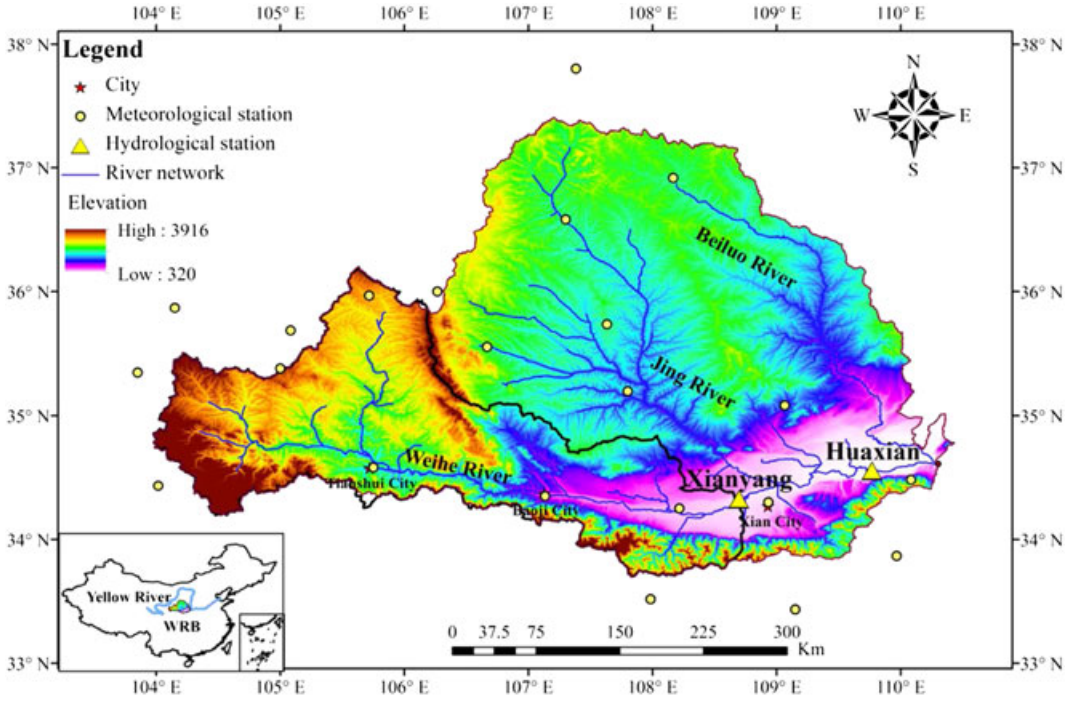

Figure 3. Location map of the river system, meteorological stations and Huaxian and Xianyang hydrological stations of the Weihe River basin. The inserted frame in the left corner depicts the geographical locations of the Weihe River basin and the Yellow River in the map of China

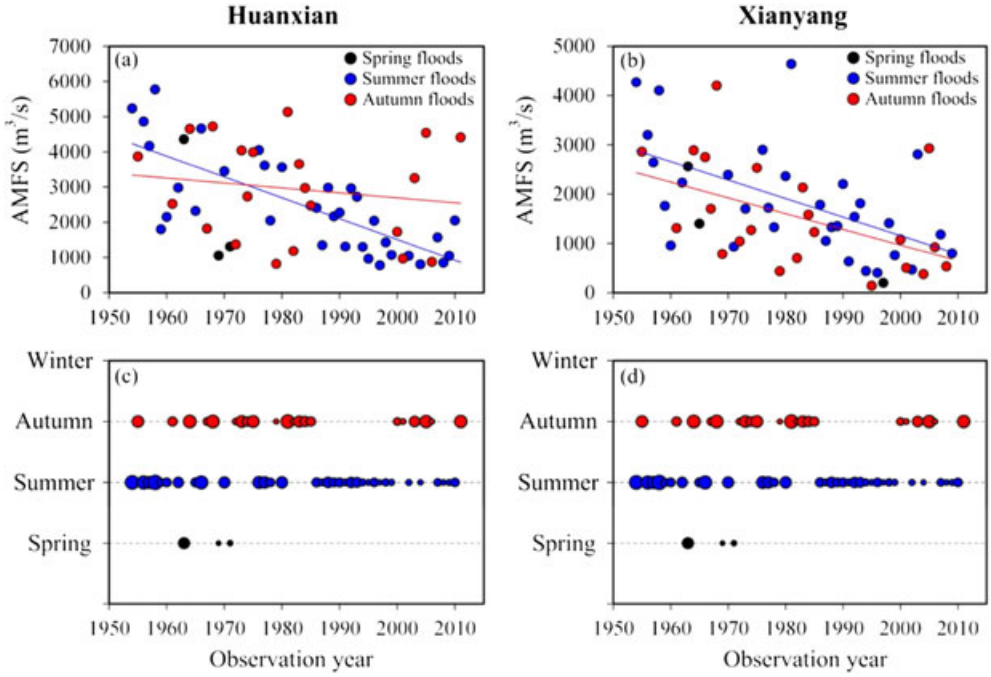

Figure 4. Preliminary analysis of seasonality of the Huaxian station (left panel) and Xianyang station (right panel). The black-filled circles represent occurrences of flood events in winter (MAM); the blue-filled circles represent occurrences of flood events in summer (JJA); the red-filled circles represent occurrences of flood events in autumn (SON); and the sizes of filled circles (bottom) represent the magnitudes of flood events, i.e. the larger the filled circle, the greater the flood event

model) and corresponding Nash–Sutcliffe efficiency (NSE) coefficient (Nash and Sutcliffe, 1970) of the optimal TTMD models are also provided.

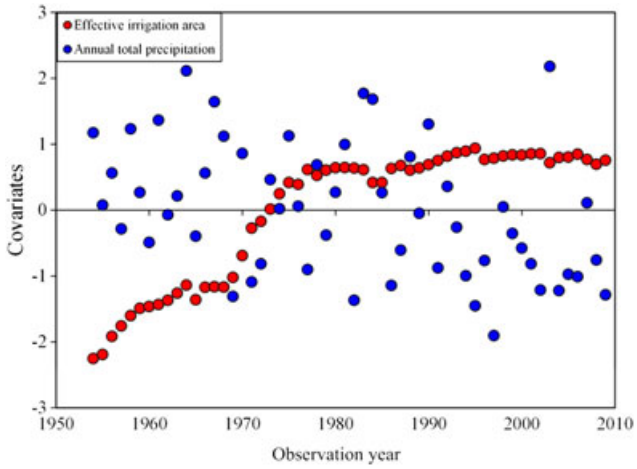

Figure 5. Time series of the two standardized covariates (effective irrigation area and annual total precipitation) used in the statistical modelling of AMFS over the period of 1954–2009 in Xianyang station

STUDY AREA AND DATA

General description of the study area

The Weihe River, which is the longest tributary of the Yellow River, originates from the Gansu province and flows through the southern Loess Plateau. The Weihe River possesses an approximate drainage area of 134 800 km^2 and has many tributaries, among which the two largest tributaries are the Jing River and Beiluo River (Figure 3). The Huaxian hydrological station, located in the most downstream of the main stream of the Weihe River, controls a drainage area about 106 321 km^2. The Xianyang station, located in 120 km upstream of Huaxian station, owns a drainage area about 47 504 km^2 (Figure 3).

The WRB being located in the region transitioning from semi-humid to semi-arid and influenced by the typical temperate continental monsoon climate, the annual total precipitation exhibits significant spatial and seasonal variations. The terrain of region controlled by Xianyang and Huaxian stations is complicated, including loess hills with a highest altitude of 3416 m above mean sea level and Guanzhong basin (320–800 m above mean sea level). Complicated terrains and corresponding land-cover types

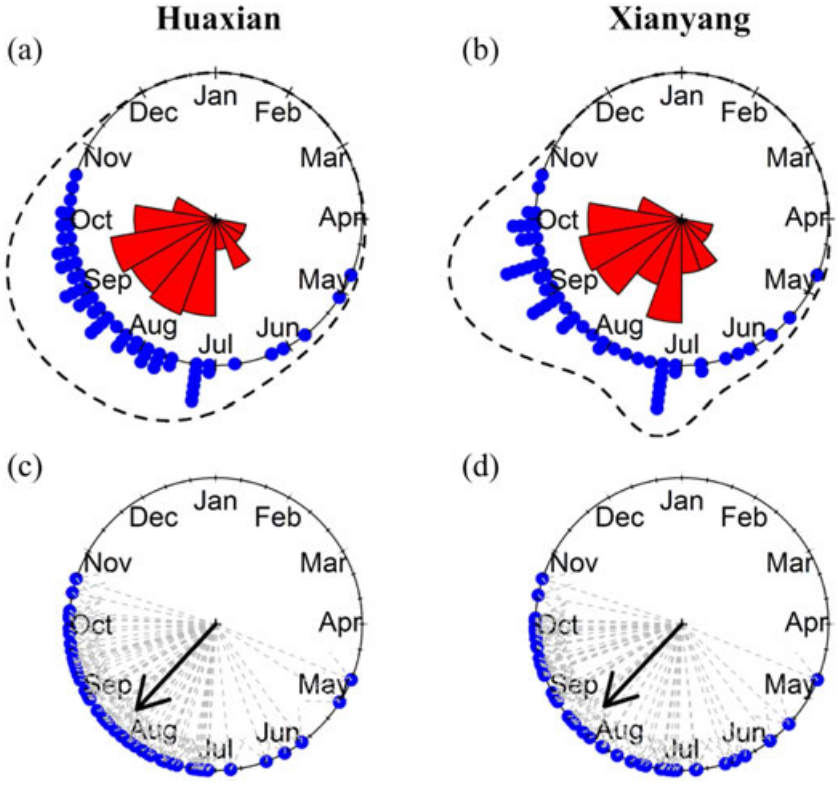

Figure 6. Graphical representations of circular data for Huaxian (left panel) and Xianyang (right panel) stations. Top panels: plots of circular statistics to characterize the seasonality of annual maximum flood events for both stations. The blue points around the circle represent the raw circular data; the red wedges in the circles are the rose diagrams; and the black dashed lines surrounding the circles are the estimated kernel density curves. Bottom panels: circular plots of the direction of each annual maximum flood event for both Huaxian and Xianyang stations. The blue points on the circle represent the raw circular data; the gray dashed arrows pointing to them represent their unit vector; and the black solid arrows represent the mean resultant vector $\bar{r}$

can result in distinct flood-generating mechanisms, together with different storm types in different seasons.

To examine distinct flood-generating mechanisms in the WRB, a preliminary assessment of seasonality was conducted as carried out by Dhakal *et al.* (2015) based on an examination of total number of annual maximum flood events that occur in four fixed seasons, i.e. winter (DJF), spring (MAM), summer (JJA) and autumn (SON), over the past 1954–2011 and 1954–2009 periods for Huaxian and Xianyang stations, respectively (Figure 4). It can be seen that the majority of annual maximum flood events occurred in summer and autumn in both Huaxian (58.6% for summer and 36.2% for autumn) and Xianyang (43.1% for summer and 51.7% for autumn) stations, exhibiting clear seasonal clustering. The results of preliminary assessment of seasonality may verify the existence of distinct flood-generating mechanisms before more robust seasonality analysis is conducted. Besides, decreasing trend can be seen in each season from Figure 4.

Table II. Results of seasonality analyses in Huaxian and Xianyang stations based on the circular statistical analysis.

Stations	Basic circular statistics		Tests for uniformity				Tests for symmetry
	$\overline{\theta}$ (radians)	$\overline{r}$	Rayleigh	Kuiper	Watson	Rao spacing	Asymptotic theory-based test
Huaxian	3.89 (13 August)	0.80	0.796**	4.73**	2.04**	212.41**	0.087*
Xianyang	3.90 (14 August)	0.77	0.771**	4.48**	1.84**	211.48**	0.046**

The zero direction is at $\pi/2$ radians from the mathematical origin corresponding to the positive horizontal axis.
*Denotes $0.05 < p\text{-value} < 0.1$;
**Denotes p-value <0.05.

Table III. Summary of the performance of the optimal time-varying single-type distributions considering different variation types and explanatory variables for each kind of distribution in modelling the AMFS from Huaxian station and Xianyang station.

Stations	Distributions		Explanatory variables		
			Time	Physical variables	Stationarity
Huaxian	Lognormal	Variation	$\mu \sim t$	$\mu \sim ia + prec$	$\mu \sim 1$
		Types	$\sigma \sim 1$	$\sigma \sim 1$	$\sigma \sim 1$
		AIC	986.14	**962.26**	1001.77
		SBC	992.32	**970.50**	1005.89
	Gamma	Variation	$\mu \sim t$	$\mu \sim ia + prec$	$\mu \sim 1$
		Types	$\sigma \sim t$	$\sigma \sim 1$	$\sigma \sim 1$
		AIC	986.06	965.51	1000.29
		SBC	994.30	973.75	1004.41
	Weibull	Variation	$\mu \sim t$	$\mu \sim ia + prec$	$\mu \sim 1$
		Types	$\sigma \sim t$	$\sigma \sim ia + prec$	$\sigma \sim 1$
		AIC	**985.00**	968.99	1000.40
		SBC	**993.24**	981.35	1004.52
Xianyang	Lognormal	Variation	$\mu \sim t$	$\mu \sim ia + prec$	$\mu \sim 1$
		Types	$\sigma \sim t$	$\sigma \sim ia + prec$	$\sigma \sim 1$
		AIC	916.64	**894.18**	938.29
		SBC	924.74	**906.33**	942.34
	Gamma	Variation	$\mu \sim t$	$\mu \sim ia + prec$	$\mu \sim 1$
		Types	$\sigma \sim t$	$\sigma \sim ia + prec$	$\sigma \sim 1$
		AIC	**914.84**	894.69	932.72
		SBC	**922.94**	906.84	936.77
	Weibull	Variation	$\mu \sim t$	$\mu \sim ia + prec$	$\mu \sim 1$
		Types	$\sigma \sim t$	$\sigma \sim ia + prec$	$\sigma \sim 1$
		AIC	915.99	895.56	932.39
		SBC	924.09	907.70	936.44

The most optimal model with time or physically-based covariates is highlighted in bold. Stationarity in the last column means the situation where distribution parameters do not vary with explanatory variables.

The WRB is the homeland of about 20 million people; besides, it is one of the most important industrial and agricultural production zones in China. Consequently, human activities, such as urbanization, river regulation and particularly the irrigated agriculture, have great effects on the hydrological processes in the WRB (Yu *et al*., 2014b). In recent decades, both the low flow and peak flow of the WRB have exhibited significant decreasing trends (Song *et al*., 2007; Xiong *et al*., 2015b; Yu *et al*., 2014a; Zuo *et al*., 2014). Du *et al.* (2015) and Xiong *et al.* (2014) studied the nonstationarity of streamflow in the WRB using time-varying single-type distributions.

Data

The observed AMFS (defined as annual maximum daily streamflow) for the period of 1954–2011 and 1954–2009 are collected from the Huaxian and Xianyang hydrological stations, respectively. Besides, two physically-based covariates, i.e. annual total precipitation (*prec*) and effective irrigation area (*ia*), are used to model the variation of AMFS of the WRB, because both climate factors and agricultural practices are considered to have significant implications on the hydrological responses to both low flow and peak flow (Juckem *et al*., 2008; Villarini and Strong, 2014).

Precipitation is used to assess the impacts of meteorological factors on the variations of AMFS. Observed daily total precipitation of the 22 meteorological stations located in the WRB is obtained from the National Climate Center of China Meteorological Administration (http://cdc.cma.gov.cn). These data are aggregated to basin scale using the Thiessen polygon method for Huaxian and Xianyang stations, respectively. The created areal mean daily series of precipitation are then aggregated at annual scale for the periods of 1954–2011 and 1954–2009 for Huaxian and Xianyang stations, respectively.

Irrigation area is selected to examine the impacts of agriculture practices in the WRB on the variations of AMFS. The irrigation area of the WRB has been growing over the past decades, and currently, there are seven large-scale irrigation districts in the WRB with a total irrigation area of about 4773 km^2. The large numbers of irrigation areas have great impacts on streamflow, not limited to direct water drawing, but to the decline of runoff-generating capability, due to increased evaporation. The

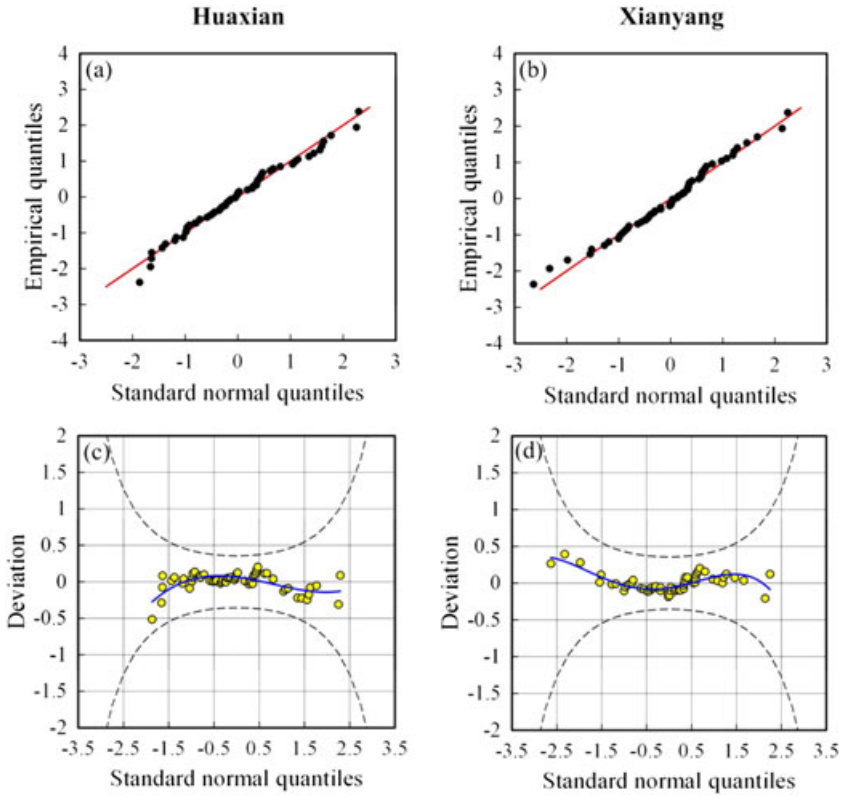

Figure 7. Diagnostic plots for evaluating the goodness-of-fit of the optimal time-varying single-type distributions for Huaxian station (left panel) and Xianyang station (right panel) using physically-based variables as covariates. (a, b) Q-Q plots based on transformation to a standard normal distribution. The red solid lines indicate 1 : 1 line (a good model should have the data points located along the red solid line); (c, d) worm plots (a good model should have the yellow data points located within the 95% confidence intervals depicted by the two black dashed lines)

data of effective irrigation area are available in annals of statistics for agriculture provided by the Shaanxi Provincial Bureau of Statistics (http://www.shaanxitj.gov.cn/).

The two covariates are standardized by subtracting the mean and dividing by the standard deviation to eliminate the largely different scales of variation between them as carried out by Villarini and Strong (2014). Take Xianyang station as an illustration, *prec* covariate exhibits remarkable variability over the period of 1954–2009, while the *ia* covariate exhibits step increase pattern over the period of 1954–2009 (Figure 5).

APPLICATION AND RESULTS

Seasonality characterization of AMFS

In addition to the preliminary analysis of seasonality, more robust analyses were conducted following the flow chart in Figure 1. Graphical representations of circular data, especially the kernel density curve used to estimate the underlying population density, are generally considered to be insightful and helpful in visualization of clustering or seasonality. As shown in Figure 6a and b, the kernel density of Huaxian station was relatively smooth from May to October, whereas the kernel density of Xianyang station exhibited evident bimodal pattern concentrated from May to July and from August to October, directly indicating the seasonality predominated by two periods. Moreover, it confirmed the existence of two distinct populations of AMFS generated by different mechanisms.

The sample mean direction $\overline{\theta}$ and mean resultant length $\overline{r}$ can provide information about the time in which annual maximum flood events tend to occur and how strong the seasonality is. As presented in Table II and Figure 6c and d, the mean time of occurrence for Huaxian and Xianyang is 14 August and 15 August, respectively. $\overline{r}$ is big for both

Table IV. Summary of the performance of different TTMD models in modelling the AMFS from Huaxian station using time as explanatory variables.

Mixture types	Variation types of time-varying parameters			AIC	SBC
LN + WEI	$w^t \sim 1$	$\mu_i^t \sim 1$	$\sigma_i^t \sim 1$	992.57	1002.88
	$w^t \sim 1$	$\mu_i^t \sim t$	$\sigma_i^t \sim 1$	985.27	999.69
	$w^t \sim 1$	$\mu_i^t \sim 1$	$\sigma_i^t \sim t$	1003.70	1017.90
	$w^t \sim 1$	$\mu_i^t \sim t$	$\sigma_i^t \sim t$	978.80	997.34
	$w^t \sim t$	$\mu_i^t \sim 1$	$\sigma_i^t \sim 1$	982.04	994.40
	$w^t \sim t$	$\mu_i^t \sim t$	$\sigma_i^t \sim 1$	979.50	995.99
	$w^t \sim t$	$\mu_i^t \sim 1$	$\sigma_i^t \sim t$	987.30	1003.79
	$w^t \sim t$	$\mu_i^t \sim t$	$\sigma_i^t \sim t$	**975.64**	**994.25**
GA + LN	$w^t \sim 1$	$\mu_i^t \sim 1$	$\sigma_i^t \sim 1$	995.61	1005.91
	$w^t \sim 1$	$\mu_i^t \sim t$	$\sigma_i^t \sim 1$	983.83	998.25
	$w^t \sim 1$	$\mu_i^t \sim 1$	$\sigma_i^t \sim t$	997.36	1011.78
	$w^t \sim 1$	$\mu_i^t \sim t$	$\sigma_i^t \sim t$	978.59	996.82
	$w^t \sim t$	$\mu_i^t \sim 1$	$\sigma_i^t \sim 1$	983.16	995.52
	$w^t \sim t$	$\mu_i^t \sim t$	$\sigma_i^t \sim 1$	987.49	1003.98
	$w^t \sim t$	$\mu_i^t \sim 1$	$\sigma_i^t \sim t$	988.06	1004.54
	$w^t \sim t$	$\mu_i^t \sim t$	$\sigma_i^t \sim t$	**976.21**	**996.82**
GA + WEI	$w^t \sim 1$	$\mu_i^t \sim 1$	$\sigma_i^t \sim 1$	992.94	1003.25
	$w^t \sim 1$	$\mu_i^t \sim t$	$\sigma_i^t \sim 1$	982.68	997.10
	$w^t \sim 1$	$\mu_i^t \sim 1$	$\sigma_i^t \sim t$	996.89	1011.31
	$w^t \sim 1$	$\mu_i^t \sim t$	$\sigma_i^t \sim t$	978.29	996.83
	$w^t \sim t$	$\mu_i^t \sim 1$	$\sigma_i^t \sim 1$	983.07	995.43
	$w^t \sim t$	$\mu_i^t \sim t$	$\sigma_i^t \sim 1$	983.79	1000.27
	$w^t \sim t$	$\mu_i^t \sim 1$	$\sigma_i^t \sim t$	987.25	1003.73
	$w^t \sim t$	$\mu_i^t \sim t$	$\sigma_i^t \sim t$	**976.86**	**997.46**

The first distribution and second distribution in the mixture types column represent $f_1(\cdot)$ and $f_2(\cdot)$ in Equation 9, respectively. The variation types correspond to the eight scenarios presented in Figure 2, and the first row in each mixture type represents the performance of stationary mixture distributions. ~ 1 and $\sim t$ denote that weighting coefficient w^t and component distributions' parameters (location μ_i^t and scale σ_i^t parameters ($i = 1,2$)) are constant and varying with time, respectively. The optimal model with the smallest AIC and SBC values for each mixture type is highlighted in bold.

Table V. Summary of the performance of different TTMD models in modelling the AMFS from Xianyang station using time as explanatory variables.

Mixture types	Variation types of time-varying parameters			AIC	SBC
LN + WEI	$w^t \sim 1$	$\mu_i^t \sim 1$	$\sigma_i^t \sim 1$	937.84	947.97
	$w^t \sim 1$	$\mu_i^t \sim t$	$\sigma_i^t \sim 1$	922.16	936.34
	$w^t \sim 1$	$\mu_i^t \sim 1$	$\sigma_i^t \sim t$	937.69	951.87
	$w^t \sim 1$	$\mu_i^t \sim t$	$\sigma_i^t \sim t$	**909.94**	**928.17**
	$w^t \sim t$	$\mu_i^t \sim 1$	$\sigma_i^t \sim 1$	923.69	935.84
	$w^t \sim t$	$\mu_i^t \sim t$	$\sigma_i^t \sim 1$	922.39	938.59
	$w^t \sim t$	$\mu_i^t \sim 1$	$\sigma_i^t \sim t$	923.02	939.22
	$w^t \sim t$	$\mu_i^t \sim t$	$\sigma_i^t \sim t$	921.29	941.54
GA + LN	$w^t \sim 1$	$\mu_i^t \sim 1$	$\sigma_i^t \sim 1$	938.00	948.13
	$w^t \sim 1$	$\mu_i^t \sim t$	$\sigma_i^t \sim 1$	921.78	935.96
	$w^t \sim 1$	$\mu_i^t \sim 1$	$\sigma_i^t \sim t$	936.15	950.33
	$w^t \sim 1$	$\mu_i^t \sim t$	$\sigma_i^t \sim t$	**911.02**	**929.25**
	$w^t \sim t$	$\mu_i^t \sim 1$	$\sigma_i^t \sim 1$	922.75	934.90
	$w^t \sim t$	$\mu_i^t \sim t$	$\sigma_i^t \sim 1$	922.56	938.76
	$w^t \sim t$	$\mu_i^t \sim 1$	$\sigma_i^t \sim t$	923.16	939.37
	$w^t \sim t$	$\mu_i^t \sim t$	$\sigma_i^t \sim t$	915.43	935.69
GA + WEI	$w^t \sim 1$	$\mu_i^t \sim 1$	$\sigma_i^t \sim 1$	937.57	947.70
	$w^t \sim 1$	$\mu_i^t \sim t$	$\sigma_i^t \sim 1$	921.81	935.99
	$w^t \sim 1$	$\mu_i^t \sim 1$	$\sigma_i^t \sim t$	935.15	949.32
	$w^t \sim 1$	$\mu_i^t \sim t$	$\sigma_i^t \sim t$	**900.24**	**918.47**
	$w^t \sim t$	$\mu_i^t \sim 1$	$\sigma_i^t \sim 1$	923.21	935.37
	$w^t \sim t$	$\mu_i^t \sim t$	$\sigma_i^t \sim 1$	922.90	939.11
	$w^t \sim t$	$\mu_i^t \sim 1$	$\sigma_i^t \sim t$	923.50	939.71
	$w^t \sim t$	$\mu_i^t \sim t$	$\sigma_i^t \sim t$	921.32	941.57

The first distribution and second distribution in the mixture types column represent $f_1(\cdot)$ and $f_2(\cdot)$ in Equation 9, respectively. The variation types correspond to the eight scenarios presented in Figure 2, and the first row in each mixture type represents the performance of stationary mixture distributions. ~ 1 and $\sim t$ denote that weighting coefficient w^t and component distributions' parameters (location μ_i^t and scale σ_i^t parameters ($i = 1,2$)) are constant and varying with time, respectively. The optimal model with the smallest AIC and SBC values for each mixture type is highlighted in bold.

Table VI. Summary of estimated parameters of the optimal TTMD models fitted to the AMFS of Huaxian and Xianyang stations using time or physically-based variables as covariates.

Optimal model	w^t	μ_1^t	σ_1^t	μ_2^t	σ_2^t
Huaxian station					
LN + WEI[a]	$\varepsilon_0 = 0.563$*	$\alpha_{10} = 8.636$***	$\beta_{10} = -5.000$***	$\alpha_{20} = 8.456$***	$\beta_{20} = 1.364$***
(t)	$\varepsilon_1 = 0.090$**	$\alpha_{11} = -0.074$***	$\beta_{11} = 0.001$*	$\alpha_{21} = -0.016$***	$\beta_{21} = -0.016$***
GA + WEI[b]	$\varepsilon_0 = 0.125$*	$\alpha_{10} = 7.579$***	$\beta_{10} = -1.446$***	$\alpha_{20} = 8.234$***	$\beta_{20} = 1.500$***
(*ia* and *prec*)	$\varepsilon_1 = -0.265$*	$\alpha_{11} = -0.233$***	—	$\alpha_{21} = -0.074$*	—
	$\varepsilon_2 = 1.601$*	$\alpha_{12} = 0.411$***	—	$\alpha_{22} = 0.063$*	—
Xianyang station					
GA + WEI[c]	$\varepsilon_0 = -2.250$***	$\alpha_{10} = 8.130$***	$\beta_{10} = -0.827$***	$\alpha_{20} = 6.996$***	$\beta_{20} = 2.895$***
(t)	—	$\alpha_{11} = -0.029$***	$\beta_{11} = 0.007$*	$\alpha_{21} = 0.019$***	$\beta_{21} = -0.075$***
GA + WEI[d]	$\varepsilon_0 = 0.098$**	$\alpha_{10} = 7.590$***	$\beta_{10} = -1.178$***	$\alpha_{20} = 7.125$***	$\beta_{20} = 1.500$***
(*ia* and *prec*)	—	$\alpha_{11} = -0.159$***	$\beta_{11} = 0.917$***	$\alpha_{21} = -0.081$*	$\beta_{21} = -0.025$***
	—	$\alpha_{12} = 0.360$***	$\beta_{12} = -0.196$*	$\alpha_{22} = 0.367$***	$\beta_{22} = 0.098$**

μ_1^t and σ_1^t are the distribution parameters belonging to the first component distribution, while μ_2^t and σ_2^t are the distribution parameters belonging to the second component distribution.
*Denotes $0.05 < p$-value < 0.1;
**Denotes $0.001 < p$-value < 0.05;
***Denotes p-value < 0.001.
[a] In the optimal TTMD model of LN and WEI with time covariate for Huaxian station, $w^t = 1/(1+\exp(\varepsilon_0 + \varepsilon_1 \times t))$; $\mu_1^t = \alpha_{10} + \alpha_{11} \times t$, $\ln(\mu_2^t) = \alpha_{20} + \alpha_{21} \times t$; $\ln(\sigma_i^t) = \beta_{i0} + \beta_{i1} \times t$ $(i = 1,2)$.
[b] In the optimal TTMD model of GA and WEI with physically-based covariates for Huaxian station, $w^t = 1/(1+\exp(\varepsilon_0 + \varepsilon_1 \times ia + \varepsilon_2 \times prec))$; $\ln(\mu_i^t) = \alpha_{i0} + \alpha_{i1} \times ia + \alpha_{i2} \times prec$ $(i = 1,2)$, $\ln(\sigma_i^t) = \beta_{i0}$ $(i = 1,2)$.
[c] In the optimal TTMD model of GA and WEI with time covariate for Xianyang station, $w^t = 1/(1+\exp(\varepsilon_0))$; $\ln(\mu_i^t) = \alpha_{i0} + \alpha_{i1} \times t$ $(i = 1,2)$; $\ln(\sigma_i^t) = \beta_{i0} + \beta_{i1} \times t$ $(i = 1,2)$.
[d] In the optimal TTMD model of GA and WEI with physically-based covariates for Xianyang station, $w^t = 1/(1+\exp(\varepsilon_0))$; $\ln(\mu_i^t) = \alpha_{i0} + \alpha_{i1} \times ia + \alpha_{i2} \times prec$ $(i = 1,2)$; $\ln(\sigma_i^t) = \beta_{i0} + \beta_{i1} \times ia + \beta_{i2} \times prec$ $(i = 1,2)$.

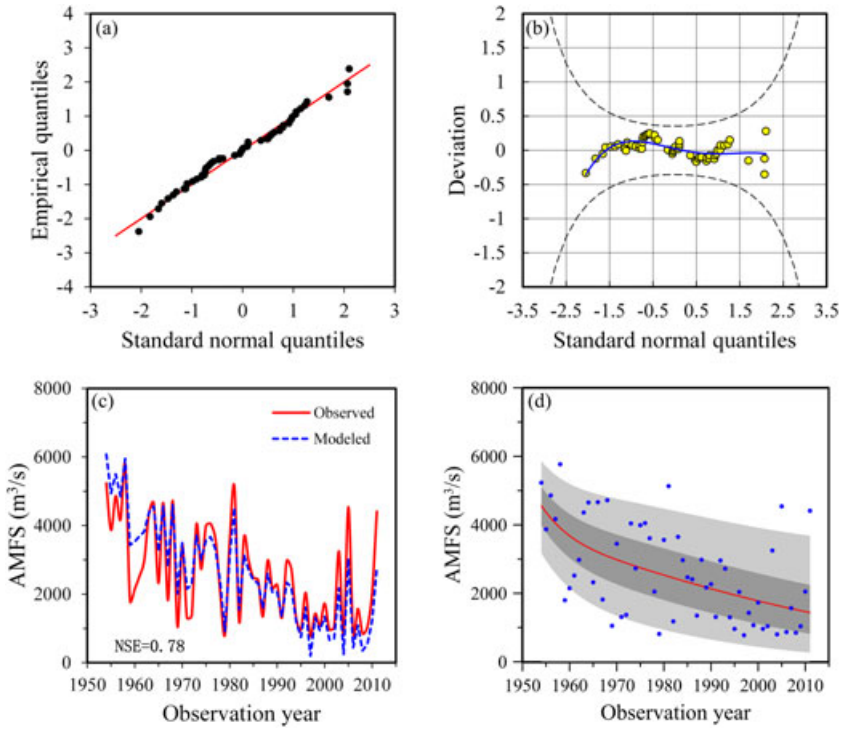

Figure 8. Diagnostic plots for evaluating the goodness-of-fit of the optimal TTMD with time covariate for Huaxian station. (a) Q-Q plots based on transformation to a standard normal distribution and the red solid lines indicate 1 : 1 line (a good model should have the data points located along the red solid line); (b) worm plot (a good model should have the yellow data points located within the 95% confidence intervals depicted by the two black dashed lines); (c) observed (red solid line) and modelled (blue dashed line) time series; (d) centiles curve plot (the blue scatters are the observed AMFS, the red line in the central is the 50% centile curve, the light grey area is the region between 5% and 95% centile curves and the dark grey area in the region between 25% and 75% centile curves. Theoretically, a good model should have the probabilities of the scatters located in light grey region and dark grey region be 90% and 50%, respectively)

Huaxian and Xianyang stations, indicating strong seasonality.

According to the results of statistical inferences (Table II) conducted to analyse the type of circular model, the null hypotheses of uniformity are rejected for both Huaxian and Xianyang stations at 0.05 significance level based on the four statistical tests (i.e. Rayleigh, Kuiper, Watson and Rao spacing tests). Then asymptotic theory-based test for reflective symmetric models was conducted, because the sample sizes of both stations were larger than 50. As shown in Table II, the null hypotheses of reflective symmetry were rejected at the 0.1 significance level for both stations. Therefore, the seasonality types in both Huaxian and Xianyang were identified as asymmetry or multimodal models (i.e. finite mixtures of unimodal symmetric and asymmetric models), indicating the existence of mixed populations or distinct flood-generating mechanisms in both stations.

Time-varying single-type distributions

In the nonstationary modelling with single-type distribution, statistical parameters of Lognormal, Gamma and Weibull were assumed to be either constant or time-varying according to different variation scenarios. The optimal nonstationary models for each covariate and distribution were presented in Table III. In general, the results showed that the time-varying single-type distributions with either time or physically-based covariates performed better than the stationary single-type distributions. Furthermore, the time-varying single-type distributions with physically-based covariates, which had smaller AIC and SBC values, were superior to those with time covariate. For Huaxian station, according to the values of AIC and SBC, the Weibull distribution (both location and scale parameters were time-varying) and the Lognormal distribution (only location parameter is time-varying) were considered as the optimal models for time and physically-based covariates, respectively, although the SBC value of optimal Weibull model was not the smallest. For Xianyang station, the Gamma and Lognormal distributions, whose location and scale parameters were both time-varying were considered as the optimal models for time and physically-based covariates, respectively. Besides, the Q-Q plots and worm plots of optimal models with physical variables for both stations exhibited good fitting qualities (Figure 7).

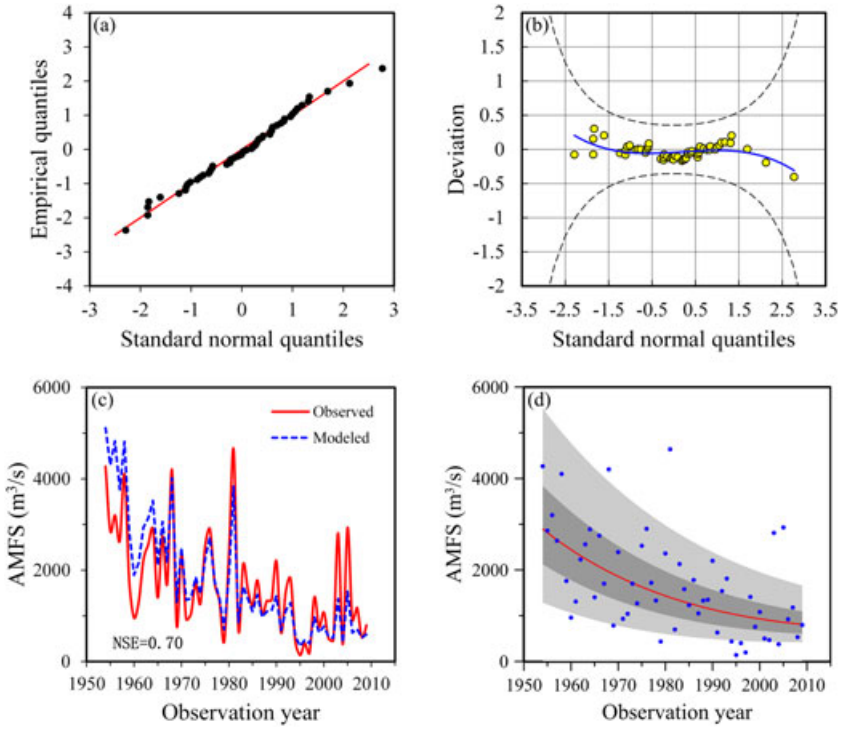

Figure 9. Diagnostic plots for evaluating the goodness-of-fit of the optimal TTMD with time covariate for Xianyang station. (a) Q-Q plots based on transformation to a standard normal distribution and the red solid lines indicate 1 : 1 line (a good model should have the data points located along the red solid line); (b) worm plot (a good model should have the yellow data points located within the 95% confidence intervals depicted by the two black dashed lines); (c) observed (red solid line) and modelled (blue dashed line) time series; (d) centiles curve plot (the blue scatters are the observed AMFS, the red line in the central is the 50% centile curve, the light grey area is the region between 5% and 95% centile curves and the dark grey area in the region between 25% and 75% centile curves. Theoretically, a good model should have the probabilities of the scatters located in light grey region and dark grey region be 90% and 50%, respectively)

Time-varying two-component mixture distributions using time as covariate

To model the nonstationary flood series in the WRB, the proposed TTMD with time covariate was applied on the basis of Equation 9. For both Huaxian and Xianyang stations, a total of 24 two-component TTMD models were built for each station considering both different mixture types of component distributions (three combinations among Lognormal, Weibull and Gamma) and the different variation types of model parameters (scenarios 1–8 in Figure 2). The time-varying parameters of TTMD were estimated by the MHML method. It was found that for both Huaxian (Table IV) and Xianyang (Table V) stations, the TTMD models with either component distributions' parameters or weighting coefficients varying with time performed better than the stationary mixture models, except for the cases in which only the scale parameter was time-varying. Furthermore, it was shown that the AIC and SBC values of these 24 mixture models were smaller than those of time-varying single-type models with time covariate as a whole, which indicated improvements of model performance.

For Huaxian station, according to AIC and SBC values, the mixture of Lognormal and Weibull was the optimal model, whose weighting coefficient w^t and component distributions' parameters, i.e. location parameter μ_i^t and scale parameter σ_i^t, were all varying with time (Table IV). For Xianyang station, the mixture of Gamma and Weibull was the optimal model, whose location parameter μ_i^t and scale parameter σ_i^t were time-varying, while the weighting coefficients were constant (Table V). The parameters of the optimal models were presented in Table VI.

For the purpose of further examination of the goodness-of-fit of the optimal model, various diagnostic plots, i.e. Q-Q plot, worm plot and centiles curve, were employed. For both stations, the scatters in the Q-Q plot

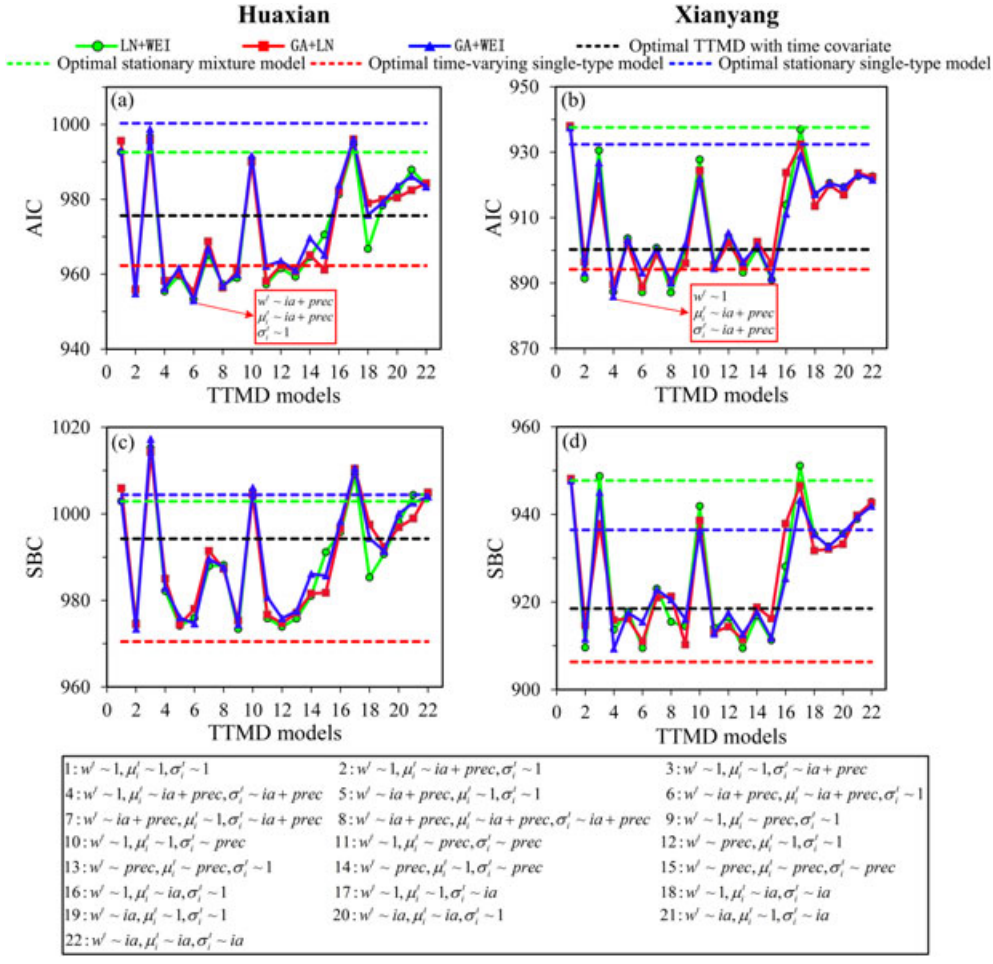

Figure 10. Summary of different TTMD models in modelling the AMFS from Huaxian station (left panel) and Xianyang station (right panel) using physically-based variables as explanatory variables. The variation types of the weighting coefficient w^t, location μ_i^t and scale σ_i^t ($i = 1,2$), corresponding to the x-axis, are shown in the black box below the figure. ~ 1 denotes that the parameters are constant, while $\sim ia + prec$, $\sim prec$ and $\sim ia$ denote that the parameters are varying with both effective irrigation area and annual total precipitation, with annual total precipitation alone and with effective irrigation area alone, respectively. The optimal TTMD models with physically-based covariates are marked by red box

aligned preferably along the red line, except for a few points in the beginning and end of the red line (Figures 8a and 9a), and all the scatters in the worm plot were within the 95% confidence interval (Figures 8b and 9b). Besides, the modelled series fitted the observed ones well for Huaxian (NSE = 0.78) and Xianyang (NSE = 0.70) stations, both indicating great agreement between the optimal model and observations. The vast majority of the points located within the region between the 5% and 95% centile curves for both stations, showing the optimal model, can model the variability of the observations (Figures 8d and 9d). The foregoing diagnostic results indicated the excellent fitting qualities of the optimal model in modelling flood series.

Time-varying two-component mixture distributions using physically-based variables as covariates

A total of 66 TTMD models with covariates of *ia* and/or *prec* were built for each station (3 stationary mixture models, 21 models for both *ia* and *prec* covariates, 21 for *ia* and 21 for *prec*). The performance of these models was summarized in Figure 10. It was found that for both stations, most of the proposed TTMD models with either component distributions' parameters or weighting coefficients varying with physically-based variables performed better than the optimal stationary mixture models and the optimal TTMD models with time covariate, in terms of both AIC and SBC values. It was also found that the overall performance of TTMD models with *prec* covariate was better than those with *ia* covariate. Besides, it should be noted that for both stations, the SBC values of the optimal time-varying single-type models with physical variables were comparable with the TTMD models with physical variables, although their AIC values were much larger than TTMD models', which indicated degradation of the performance of TTMD models with a large number of parameters.

For Huaxian station, the two-component mixture of Gamma and Weibull distributions, with weighting coefficient w^t and location parameter μ_i^t varying with *ia* and *prec*, was the optimal model according to AIC and SBC values (Figure 10). While for Xianyang station, the two-component mixture of Gamma and Weibull distributions, with location parameter μ_i^t and scale parameter σ_i^t varying with *ia* and *prec*, was the optimal model. The parameters of the optimal models were presented in Table VI. Then, further diagnosis was employed to examine the goodness-of-fit of the optimal models. The

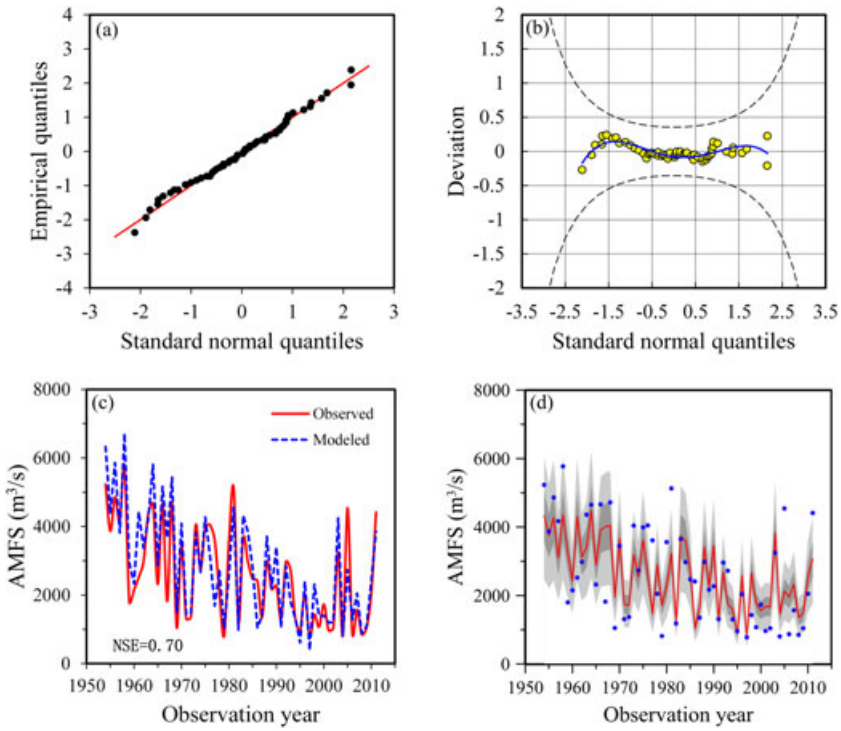

Figure 11. Diagnostic plots for evaluating the goodness-of-fit of the optimal TTMD with *ia* and *prec* covariates together for Huaxian station. (a) Q-Q plots based on transformation to a standard normal distribution and the red solid lines indicate 1 : 1 line (a good model should have the data points located along the red solid line); (b) worm plot (a good model should have the yellow data points located within the 95% confidence intervals depicted by the two black dashed lines); (c) observed (red solid line) and modelled (blue dashed line) time series; (d) centiles curve plot (the blue scatters are the observed AMFS, the red line in the central is the 50% centile curve, the light grey area is the region between 5% and 95% centile curves and the dark grey area in the region between 25% and 75% centile curves. Theoretically, a good model should have the probabilities of the scatters located in light grey region and dark grey region be 90% and 50%, respectively)

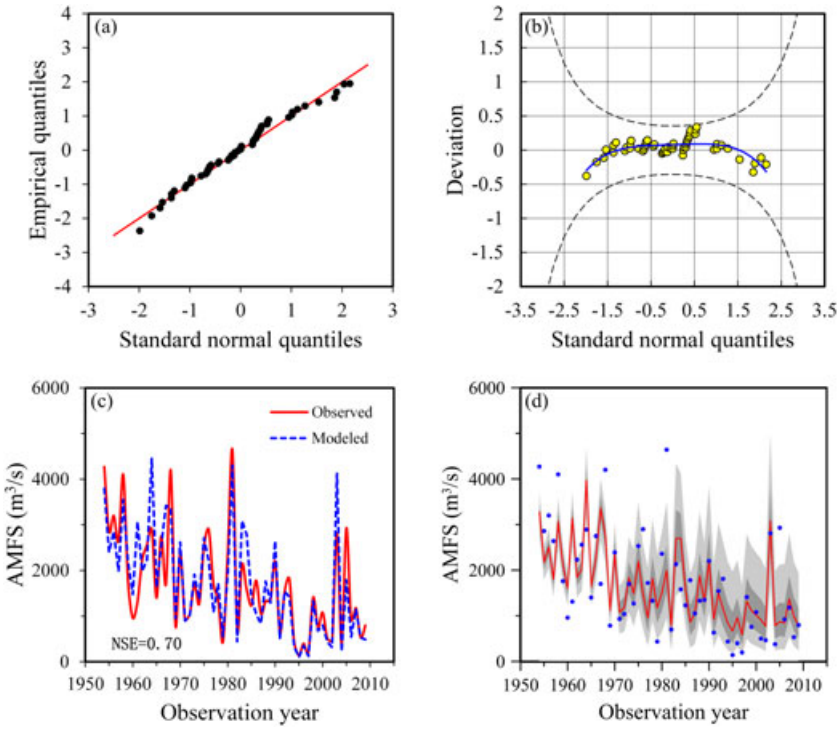

Figure 12. Diagnostic plots for evaluating the goodness-of-fit of the optimal TTMD with *ia* and *prec* covariates together for Xianyang station. (a) Q-Q plots based on transformation to a standard normal distribution and the red solid lines indicate 1 : 1 line (a good model should have the data points located along the red solid line); (b) worm plot (a good model should have the yellow data points located within the 95% confidence intervals depicted by the two black dashed lines); (c) observed (red solid line) and modelled (blue dashed line) time series; (d) centiles curve plot (the blue scatters are the observed AMFS, the red line in the central is the 50% centile curve, the light grey area is the region between 5% and 95% centile curves and the dark grey area in the region between 25% and 75% centile curves. Theoretically, a good model should have the probabilities of the scatters located in light grey region and dark grey region be 90% and 50%, respectively)

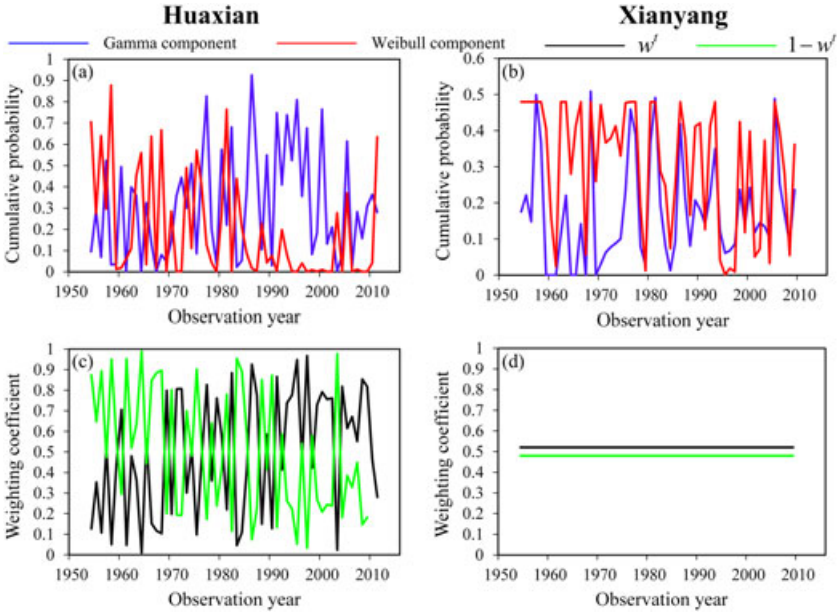

Figure 13. The evolution of cumulative probability of the Gamma component ($w^t F_1(y_t|\boldsymbol{\theta}^t)$) and Weibull component ($(1-w^t)F_2(y_t|\boldsymbol{\theta}^t)$) and of the optimal TTMD model with physically-based covariates for Huaxian station (left panel) and Xianyang station (right panel), along with the evolution of the weighting coefficients w^t and $1-w^t$ (bottom). The blue solid and black solid lines represent the cumulative probability and weighting coefficient belonging to Gamma component, respectively, while the red solid and green solid lines represent the cumulative probability and weighting coefficient belonging to Weibull component, respectively

diagnostic plots, i.e. Q-Q plot, worm plot and centile curves, exhibited good agreement between the optimal model and observations (Figures 11 and 12). Besides, the modelled series fitted the observed ones well for both Huaxian (NSE = 0.70) and Xianyang (NSE = 0.70) stations, showing good fitting qualities of the optimal models. It should be noted that the probabilistic coverage of the fifth percentile curve was not good. Future study can focus on improving the model's capability of fitting annual maxima of dry years.

To give a visual exhibition of the probability transition between the two components of the optimal models, for both stations, the cumulative probability of the Gamma component, i.e. $w^t F_1(y_t|\boldsymbol{\theta}^t)$ in Equation 10, and the Weibull component, i.e. $(1-w^t)F_2(y_t|\boldsymbol{\theta}^t)$ in Equation 10 (Figure 13a and b), along with the evolution of the weighting coefficients w^t and $1-w^t$ (Figure 13c and d), were presented. For Huaxian station, the results showed that the cumulative probability of Gamma component fluctuated dramatically for the period of 1954–2011 and showed an upward trend, while the cumulative probability of the Weibull component exhibited a downward trend. Meanwhile, the weighting coefficients varied from year to year significantly. For Xianyang station, the cumulative probabilities of Gamma and Weibull components fluctuated less dramatically than those for Huaxian station, with constant weighting coefficients of 0.52 and 0.48, respectively. It should be noted that the estimated weighting coefficients were similar to the percentages of flood events occurred in summer (0.43) and autumn (0.53) calculated in preliminary analysis of seasonality, indicating satisfactory capture of distinct flood populations.

The different variation types of the optimal TTMD models for Huaxian and Xianyang stations can be attributed to the complicated terrain (e.g. loess hills and basin topography) and temporal–spatial variation of rainfall across the WRB. The terrain controlled by Xianyang is complicated, and its response to rainfall is more rapid and significant than Huaxian whose drainage area is about double of Xianyang with inflow from Jing River (Figure 3).

CONCLUSIONS AND DISCUSSIONS

To address the variation issue of either statistical parameters or distribution types in the nonstationary flood frequency analysis and provide a flexible tool allowing for all scenarios, the TTMD model was proposed in this study. The proposed TTMD model was based on the mixture distributions and the time-varying moments method. Both the component distributions' parameters and weighting coefficients of TTMD were assumed to have a linear or non-linear trend with explanatory variables such as time or physically-based variables in the framework of time-varying moments method. Besides, to estimate the parameters of the TTMD model, whose amount is larger as compared with other distributions, an estimation approach was also employed by incorporating SAA and MLE in the framework of MHML. The main conclusions of this study were drawn as follows.

(1) The mixed populations or distinct flood-generating mechanisms were identified for both Huaxian and Xianyang stations through the seasonality analysis of AMFS for the period of 1954–2011 and 1954–2009, respectively, based on the preliminary analysis and circular statistics. Although both stations exhibited asymmetric pattern of seasonality, the seasonality of Xianyang station was more significant (with a smaller *p*-value) and closer to bimodal model compared with that of Huaxian station.
(2) In general, the proposed TTMD models exhibited good fitting qualities and outperformed the stationary single-type distributions, stationary mixture distributions and time-varying single-type distributions in modelling the AMFS of both Huaxian and Xianyang stations in the WRB, indicating the advantages of considering variations of either statistical parameters or distribution types in the nonstationary flood frequency analysis. Meanwhile, it should be noted that the TTMD models contained more parameters than other models, which would restrict their applications to some degree.
(3) According to AIC and SBC values, for Huaxian station, the two-component mixture of Gamma and Weibull distributions was the optimal model (scale parameter σ_i^t was constant, while weighting coefficient w^t and location parameter μ_i^t varied with *ia* and *prec*), whereas for Xianyang station, the mixture of Gamma and Weibull distributions with constant weighting coefficients and time-varying distribution parameters (with *ia* and *prec* covariates) was the optimal model. The different variation types resulted from the different drainage areas of the two stations, together with complicated terrain and temporal–spatial variation of rainfall across the WRB. Besides, the constant and time-varying weighting coefficients of the two optimal TTMD models indicated the existence of changing or constant probability transition between distinct flood populations. For Xianyang station, the constant weighting coefficients were similar to the percentages of different populations represented by fixed seasons, indicating satisfactory capture of distinct flood populations.
(4) It was also found that when performing nonstationary frequency analysis with either time-varying single-

type or TTMD, the performance of models with physical covariates was better than those with time covariate, indicating the superiority of using physically-based covariates as explanatory variables in nonstationary flood frequency analysis. Moreover, it was also found that the explanatory power of *prec* was better than *ia*, because of its large variation type.

The aforementioned results confirmed the physical mechanism of the utilization of mixture distributions and highlighted the advantages of using TTMD models and physically-based covariates in nonstationary flood frequency analysis. However, there are still several comments that should be made as follows.

First, it should be emphasized that for a watershed, different flood-generating mechanisms would lead to distinct flood populations, and mixture distributions are effective tools to model these mixed flood populations. Meanwhile, under changing environments due to climate change or human activities, either the distributions (type or parameters) used to describe the statistical characteristics of each flood population or the occurrence probabilities of each flood-generating mechanism (i.e. weighting coefficients of mixture distributions) are prone to change. To fully take account of all possible causes leading to the heterogeneity or nonstationarity of AMFS, we need a frequency analysis model considering the temporal changes not only in the weighting coefficients of distinct flood populations but also in the statistical types or parameters of each flood population. Thus, the frequency analysis model of TTMD is proposed in this paper to further our physical understanding of changing nature of flooding.

Second, it is worth noting that it should be more cautious to perform the nonstationary frequency analysis, considering the difficulties of obtaining credible future predictions. Indeed, many hydrological time series can be considered as a combination of deterministic and stationary stochastic components. Thus, change does not certainly imply nonstationarity, and stationarity cannot be simply interpreted as at all unchanging process state (Montanari and Koutsoyiannis, 2014; Serinaldi and Kilsby, 2015). Therefore, nonstationarity cannot be informed only in the view of statistics of observations but should be comprehensively confirmed by the combination of climatic factors analysis, attribution analysis, statistical analysis and empirical analysis (Milly *et al*., 2015). To manage the challenges from the intensive extreme events and the increased failure risk of hydraulic engineering under changing environments, new approaches that can improve the evaluation of both the deterministic and stochastic components of the hydrologic system by combining the physically-based models and statistical models should be pursued.

Third, as discussed by other researchers, in the application of the mixture distributions, two challenging problems need to be settled. Above all, one must make decisions about the number of the component distributions, which depend largely on the number of mixed populations and the stability of the parameter estimation method. In this study, having detected two predominant seasons of floods, mixture distributions with only two components were established. In future, a more robust parameter estimation method should be studied for cases with more complicated mixture nature. Another problem is the determination of appropriate frequency distributions for components of TTMD. Although the component distributions were selected on the basis of categories of popular extreme distributions in the flood frequency analysis in this study, subjectivity still exists in the choice of distributions. Consequently, more research about selection of flood frequency distributions, considering the physical processes of hydrological events and tail behaviour of distributions, should be made.

Fourth, it should also be noted that although two physically-based covariates, i.e. *prec* and *ia*, were employed to describe the time-varying characters of the weighting coefficients and component distributions' parameters in the proposed TTMD models, the explanatory power of *ia* alone was not good enough. It would be more convincing to use covariates that have stronger explanatory power and clearer physical connections with flood events in future research. In addition, although it was limited to mixture of Lognormal, Gamma and Weibull distributions for illustration purpose in this study, the proposed model is a flexible tool that can be extended to other widely used two-parameter or three-parameter extreme value distributions in flood frequency analysis.

ACKNOWLEDGEMENTS

This research is financially supported by the National Natural Science Foundation of China (NSFC Grants 51525902, 51190094 and 51479139), which are greatly appreciated. Great thanks are due to the editor and two reviewers, as their comments are all valuable and very helpful for improving the quality of this paper.

REFERENCES

Akaike H. 1974. A new look at the statistical model identification. *IEEE Transactions on Automatic Control* **19**(6): 716–723. DOI:10.1109/TAC.1974.1100705

Alila Y, Mtiraoui A. 2002. Implications of heterogeneous flood-frequency distributions on traditional stream-discharge prediction techniques. *Hydrological Processes* **16**(5): 1065–1084. DOI:10.1002/hyp.346

Black AR, Werritty A. 1997. Seasonality of flooding: a case study of North Britain. *Journal of Hydrology* **195**(1): 1–25. DOI:10.1016/S0022-1694(96)03264-7

Burn DH. 1997. Catchment similarity for regional flood frequency analysis using seasonality measures. *Journal of Hydrology* **202**(1): 212–230. DOI:10.1016/S0022-1694(97)00068-1

Cannon AJ. 2010. A flexible nonlinear modelling framework for nonstationary generalized extreme value analysis in hydroclimatology. *Hydrological Processes* **24**(6): 673–685. DOI:10.1002/hyp.7506

Černý V. 1985. Thermodynamical approach to the traveling salesman problem: an efficient simulation algorithm. *Journal of Optimization Theory and Applications* **45**(1): 41–51. DOI:10.1007/BF00940812

Chen L, Guo S, Yan B, Liu P, Fang B. 2010. A new seasonal design flood method based on bivariate joint distribution of flood magnitude and date of occurrence. *Hydrological Sciences Journal – Journal des Sciences Hydrologiques* **55**(8): 1264–1280. DOI:10.1080/02626667.2010.520564

Chen L, Singh VP, Guo S, Fang B, Liu P. 2013. A new method for identification of flood seasons using directional statistics. *Hydrological Sciences Journal* **58**(1): 28–40. DOI:10.1080/02626667.2012.743661

Condon LE, Gangopadhyay S, Pruitt T. 2015. Climate change and non-stationary flood risk for the Upper Truckee River Basin. *Hydrology and Earth System Sciences* **19**(1): 159–175. DOI:10.5194/hess-19-159-2015

Cunderlik JM, Ouarda TB, Bobée B. 2004. Determination of flood seasonality from hydrological records/Détermination de la saisonnalité des crues à partir de séries hydrologiques. *Hydrological Sciences Journal* **49**(3): DOI:10.1623/hysj.49.3.511.54351

De Michele C, Rosso R. 2002. A multi-level approach to flood frequency regionalisation. *Hydrology and Earth System Sciences Discussions* **6**(2): 185–194. DOI:10.5194/hess-6-185-2002

Dhakal N, Jain S, Gray A, Dandy M, Stancioff E. 2015. Nonstationarity in seasonality of extreme precipitation: a nonparametric circular statistical approach and its application. *Water Resources Research* **51**(6): 4499–4515. DOI:10.1002/2014WR016399

Dowsland KA, Thompson JM. 2012. Simulated annealing. In *Handbook of Natural Computing*. Springer: Berlin; 1623–1655.

Du T, Xiong L, Xu CY, Gippel CJ, Guo S, Liu P. 2015. Return period and risk analysis of nonstationary low-flow series under climate change. *Journal of Hydrology* **527**: 234–250. DOI:10.1016/j.jhydrol.2015.04.041

El Adlouni S, Bobée B, Ouarda TBMJ. 2008. On the tails of extreme event distributions in hydrology. *Journal of Hydrology* **355**(1–4): 16–33. DOI:10.1016/j.jhydrol.2008.02.011

El Adlouni S, Ouarda T, Zhang X, Roy R, Bobée B. 2007. Generalized maximum likelihood estimators for the nonstationary generalized extreme value model. *Water Resources Research* **43**(3W03410): DOI:10.1029/2005WR004545

Evin G, Merleau J, Perreault L. 2011. Two-component mixtures of normal, gamma, and Gumbel distributions for hydrological applications. *Water Resources Research* **47**(8W08525): DOI:10.1029/2010WR010266

Fiorentino M, Arora K, Singh VP. 1987. The two-component extreme value distribution for flood frequency analysis: derivation of a new estimation method. *Stochastic Hydrology and Hydraulics* **1**(3): 199–208. DOI:10.1007/BF01543891

Franks SW, Kuczera G. 2002. Flood frequency analysis: evidence and implications of secular climate variability, New South Wales. *Water Resources Research* **38**(5): 20–21. DOI:10.1029/2001WR000232

Galiatsatou P, Anagnostopoulou C, Prinos P. 2016. Modeling nonstationary extreme wave heights in present and future climates of Greek Seas. *Water Science and Engineering* **9**(1): 21–32. DOI:10.1016/j.wse.2016.03.001

Giraldo Osorio JD, García Galiano SG. 2012. Non-stationary analysis of dry spells in monsoon season of Senegal River Basin using data from regional climate models (RCMs). *Journal of Hydrology* **450–451**: 82–92. DOI:10.1016/j.jhydrol.2012.05.029

Grego JM, Yates PA. 2010. Point and standard error estimation for quantiles of mixed flood distributions. *Journal of Hydrology* **391**(3): 289–301. DOI:10.1016/j.jhydrol.2010.07.027

Hassanzadeh Y, Abdi A, Talatahari S, Singh VP. 2011. Meta-heuristic algorithms for hydrologic frequency analysis. *Water Resources Management* **25**(7): 1855–1879. DOI:10.1007/s11269-011-9778-1

Jiang C, Xiong L, Xu CY, Guo S. 2015. Bivariate frequency analysis of nonstationary low-flow series based on the time-varying copula. *Hydrological Processes* **29**(6): 1521–1534. DOI:10.1002/hyp.10288

Juckem PF, Hunt RJ, Anderson MP, Robertson DM. 2008. Effects of climate and land management change on streamflow in the driftless area of Wisconsin. *Journal of Hydrology* **355**(1): 123–130. DOI:10.1016/j.jhydrol.2008.03.010

Khaliq MN, Ouarda TBMJ, Ondo JC, Gachon P, Bobée B. 2006. Frequency analysis of a sequence of dependent and/or non-stationary physically-based observations: a review. *Journal of Hydrology* **329**(3–4): 534–552. DOI:10.1016/j.jhydrol.2006.03.004

Kirkpatrick S, Gelatt CD, Vecchi MP. 1983. Optimization by simulated annealing. *Science* **220**(4598): 671–680. DOI:10.1126/science.220.4598.671

Klemeš V. 1986. Dilettantism in hydrology: transition or destiny? *Water Resources Research* **22**(9S): 177S–188S. DOI:10.1029/WR022i09Sp0177S

Klemeš V. 1994. Statistics and probability: wrong remedies for a confused hydrologic modeller. In *Statistics for the Environment 2: Water Related Issues*, Barnett V, Turkman KF (eds). Wiley: Chichester, U.K.; 345–366.

Klemeš V. 2000. Tall tales about tails of hydrological distributions: I. *Journal of Hydrologic Engineering* **5**(3): 227–231. DOI:10.1061/(ASCE)1084-0699(2000)5:3(227)

Köplin N, Schädler B, Viviroli D, Weingartner R. 2014. Seasonality and magnitude of floods in Switzerland under future climate change. *Hydrological Processes* **28**(4): 2567–2578. DOI:10.1002/hyp.9757

Koutsoyiannis D, Montanari A. 2014. Negligent killing of scientific concepts: the stationarity case. *Hydrological Sciences Journal* **60**(7-8): 1174–1183. DOI:10.1080/02626667.2014.959959

Lee T, Jeong C. 2014. Frequency analysis of nonidentically distributed hydrometeorological extremes associated with large-scale climate variability applied to South Korea. *Journal of Applied Meteorology and Climatology* **53**(5): 1193–1212. DOI:10.1175/JAMC-D-13-0200.1

Leytham KM. 1984. Maximum likelihood estimates for the parameters of mixture distributions. *Water Resources Research* **20**(7): 896–902. DOI:10.1029/WR020i007p00896

Li J, Tan S. 2015. Nonstationary flood frequency analysis for annual flood peak series, adopting climate indices and check dam index as covariates. *Water Resources Management* **29**(15): 5533–5550. DOI:10.1007/s11269-015-1133-5

Lima CHR, Lall U, Troy TJ, Devineni N. 2015. A climate informed model for nonstationary flood risk prediction: application to Negro River at Manaus, Amazonia. *Journal of Hydrology* **522**: 594–602. DOI:10.1016/j.jhydrol.2015.01.009

Lins HF, Cohn TA. 2011. Stationarity: wanted dead or alive? 1. *Journal of the American Water Resources Association* **47**(3): 475–480. DOI:10.1111/j.1752-1688.2011.00542.x

Liu D, Guo S, Lian Y, Xiong L, Chen X. 2015. Climate-informed low-flow frequency analysis using nonstationary modelling. *Hydrological Processes* **29**(9): 2112–2124. DOI:10.1002/hyp.10360

López J, Francés F. 2013. Non-stationary flood frequency analysis in continental Spanish rivers, using climate and reservoir indices as external covariates. *Hydrology and Earth System Sciences Discussions* **17**(8): 3103–3142. DOI:10.5194/hessd-10-3103-2013

Mardia KV, Jupp PE. 2000. *Directional Statistics*. John Wiley & Sons: Chichester.

Malamud BD, Turcotte DL. 2006. The applicability of power-law frequency statistics to floods. *Journal of Hydrology* **322**(1–4): 168–180. DOI:10.1016/j.jhydrol.2005.02.032

Matalas NC. 2012. Comment on the announced death of stationarity. *Journal of Water Resources Planning and Management* **138**(4): 311–312. DOI:10.1061/(ASCE)WR.1943-5452.0000215 311-312

McLachlan G, Peel D. 2000. *Finite Mixture Model*. John Wiley & Sons: New York.

Milly PCD, Betancourt J, Falkenmark M, Hirsch RM, Kundzewicz ZW, Lettenmaier DP, Stouffer RJ, Dettinger MD, Krysanova V. 2015. On critiques of "Stationarity is Dead: Whither Water Management?". *Water Resources Research* **51**(9): 7785–7789. DOI:10.1002/2015WR017408

Milly PCD, Betancourt J, Falkenmark M, Hirsch RM, Kundzewicz ZW, Lettenmaier DP, Stouffer RJ. 2008. Stationarity is dead: whither water management? *Science* **319**(5863): 573–574. DOI:10.1126/science.1151915

Montanari A, Koutsoyiannis D. 2014. Modeling and mitigating natural hazards: stationarity is immortal!. *Water Resources Research* **50**(12): 9748–9756. DOI:10.1002/2014WR016092

Montanari A, Young G, Savenije H, Hughes D, Wagener T, Ren LL, Koutsoyiannis D, Cudennec C, Toth E, Grimaldi S. 2013. "Panta Rhei – Everything Flows": change in hydrology and society – the IAHS scientific decade 2013–2022. *Hydrological Sciences Journal* **58**(6): 1256–1275. DOI:10.1080/02626667.2013.809088

Nash JE, Sutcliffe JV. 1970. River flow forecasting through conceptual models part I – a discussion of principles. *Journal of Hydrology* **10**(3): 282–290. DOI:10.1016/0022-1694(70)90255-6

Pewsey A, Neuhäuser M, Ruxton GD. 2013. *Circular Statistics in R*. Oxford University Press: Oxford.

Prosdocimi I, Kjeldsen TR, Miller JD. 2015. Detection and attribution of urbanization effect on flood extremes using nonstationary flood frequency models. *Water Resources Research* **51**(6): 4244–4262. DOI:10.1002/2015WR017065

Read LK, Vogel RM. 2015. Reliability, return periods, and risk under nonstationarity. *Water Resources Research* **51**(8): 6381–6398. DOI:10.1002/2015WR017089

Rigby RA, Stasinopoulos DM. 2005. Generalized additive models for location, scale and shape. *Journal of the Royal Statistical Society: Series C: Applied Statistics* **54**(3): 507–554. DOI:10.1111/j.1467-9876.2005.00510.x

Rossi F, Fiorentino M, Versace P. 1984. Two-component extreme value distribution for flood frequency analysis. *Water Resources Research* **20** (7): 847–856. DOI:10.1029/WR020i007p00847

Salas JD, Obeysekera J. 2013. Revisiting the concepts of return period and risk for nonstationary hydrologic extreme events. *Journal of Hydrologic Engineering* **19**(3): 554–568. DOI:10.1061/(ASCE)HE.1943-5584.0000820 554-568

Sarhadi A, Burn DH, Concepción Ausín M, Wiper MP. 2016. Time varying nonstationary multivariate risk analysis using a dynamic Bayesian copula. *Water Resources Research* **52**: 2327–2349. DOI:10.1002/2015WR018525

Schwarz G. 1978. Estimating the dimension of a model. *The Annals of Statistics* **6**(2): 461–464. DOI:10.1214/aos/1176344136

Serinaldi F, Kilsby CG. 2015. Stationarity is undead: uncertainty dominates the distribution of extremes. *Advances in Water Resources* **77**: 17–36. DOI:10.1016/j.advwatres.2014.12.013

Shin J, Heo J, Jeong C, Lee T. 2014. Meta-heuristic maximum likelihood parameter estimation of the mixture normal distribution for physically-based variables. *Stochastic Environmental Research and Risk Assessment* **28**(2): 347–358. DOI:10.1007/s00477-013-0753-7

Singh KP, Sinclair RA. 1972. Two-distribution method for flood frequency analysis. *Journal of the Hydraulics Division* **98**(1): 29–44.

Singh VP, Wang SX, Zhang L. 2005. Frequency analysis of nonidentically distributed hydrologic flood data. *Journal of Hydrology* **307**(1-4): 175–195. DOI:10.1016/j.jhydrol.2004.10.029

Sivapalan M, Blöschl G, Merz R, Gutknecht D. 2005. Linking flood frequency to long-term water balance: incorporating effects of seasonality. *Water Resources Research* **41**(6): W06012–W06028. DOI:10.1029/2004WR003439

Smith JA, Villarini G, Baeck ML. 2011. Mixture distributions and the hydroclimatology of extreme rainfall and flooding in the eastern United States. *Journal of Hydrometeorology* **12**(2): 294–309. DOI:10.1175/2010JHM1242.1

Song JX, Xu ZX, Liu CM, Li HE. 2007. Ecological and environmental instream flow requirements for the Wei River – the largest tributary of the Yellow River. *Hydrological Processes* **21**(8): 1066–1073. DOI:10.1002/hyp.6287

Stedinger JR, Vogel RM, Foufoula-Georgiou E. 1993. Frequency analysis of extreme events. In *Handbook of Hydrology*, Maidment DR (ed). McGraw-Hill: New York.

Strupczewski WG, Kochanek K, Bogdanowicz E, Markiewicz I. 2012. On seasonal approach to flood frequency modelling. Part I: two-component distribution revisited. *Hydrological Processes* **26**(5): 705–716. DOI:10.1002/hyp.8179

Strupczewski WG, Singh VP, Mitosek HT. 2001. Non-stationary approach to at-site flood frequency modelling. III. Flood analysis of Polish rivers. *Journal of Hydrology* **248**(1): 152–167. DOI:10.1016/S0022-1694(01)00399-7

US Water Resources Council (USWRC). 1981. Guidelines for determining flow frequency. Bulletin 17B, Washington, DC, USA.

van Buuren S, Fredriks M. 2001. Worm plot: a simple diagnostic device for modelling growth reference curves. *Statistics in Medicine* **20**(8): 1259–1277. DOI:10.1002/sim.746

Villarini G. 2016. On the seasonality of flooding across the continental United States. *Advances in Water Resources* **87**: 80–91. DOI:10.1016/j.advwatres.2015.11.009

Villarini G, Scoccimarro E, White KD, Arnold JR, Schilling KE, Ghosh J. 2015. Projected changes in discharge in an agricultural watershed in Iowa. *Journal of the American Water Resources Association* **51**(5): 1361–1371. DOI:10.1111/1752-1688.12318

Villarini G, Serinaldi F, Smith JA, Krajewski WF. 2009a. On the stationarity of annual flood peaks in the continental United States during the 20th century. *Water Resources Research* **45**(8W08417): DOI:10.1029/2008WR007645

Villarini G, Smith JA, Serinaldi F, Bales J, Bates PD, Krajewski WF. 2009b. Flood frequency analysis for nonstationary annual peak records in an urban drainage basin. *Advances in Water Resources* **32**(8): 1255–1266. DOI:10.1016/j.advwatres.2009.05.003

Villarini G, Smith JA. 2010. Flood peak distributions for the eastern United States. *Water Resources Research* **46**(6W06504): DOI:10.1029/2009WR008395

Villarini G, Smith JA, Napolitano F. 2010. Nonstationary modeling of a long record of rainfall and temperature over Rome. *Advances in Water Resources* **33**(10): 1256–1267. DOI:10.1016/j.advwatres.2010.03.013

Villarini G, Smith JA, Baeck ML, Krajewski WF. 2011. Examining flood frequency distributions in the midwest U.S. *Journal of the American Water Resources Association* **47**(3): 447–463. DOI:10.1111/j.1752-1688.2011.00540.x

Villarini G, Strong A. 2014. Roles of climate and agricultural practices in discharge changes in an agricultural watershed in Iowa. *Agriculture, Ecosystems & Environment* **188**: 204–211. DOI:10.1016/j.agee.2014.02.036

Vogel RM, Yaindl C, Walter M. 2011. Nonstationarity: flood magnification and recurrence reduction factors in the United States1. *Journal of the American Water Resources Association* **47**(3): 464–474. DOI:10.1111/j.1752-1688.2011.00541.x

Waylen P, Woo MK. 1982. Prediction of annual floods generated by mixed processes. *Water Resources Research* **18**(4): 1283–1286. DOI:10.1029/WR018i004p01283

Woo MK, Waylen P. 1984. Areal prediction of annual floods generated by two distinct processes. *Hydrological Sciences Journal* **29**(1): 75–88. DOI:10.1080/02626668409490923

Xiong L, Jiang C, Du T. 2014. Statistical attribution analysis of the nonstationarity of the annual runoff series of the Weihe River. *Water Science and Technology* **70**(5): 939–946. DOI:10.2166/wst.2014.322

Xiong L, Jiang C, Xu CY, Yu K, Guo S. 2015a. A framework of change-point detection for multivariate hydrological series. *Water Resources Research* **51**(10): 8198–8217. DOI:10.1002/2015WR017677

Xiong L, Du T, Xu CY, Guo S, Jiang C, Gippel CJ. 2015b. Non-stationary annual maximum flood frequency analysis using the norming constants method to consider non-stationarity in the annual daily flow series. *Water Resources Management* **29**(10): 3615–3633. DOI:10.1007/s11269-015-1019-6

Yu K, Xiong L, Gottschalk L. 2014a. Derivation of low flow distribution functions using copulas. *Journal of Hydrology* **508**: 273–288. DOI:10.1016/j.jhydrol.2013.09.057

Yu Z, Yang T, Schwartz FW. 2014b. Water issues and prospects for hydrological science in China. *Water Science and Engineering* **7**(1): 1–4. DOI:10.3882/j.issn.1674-2370.2014.01.001

Zeng H, Feng P, Li X. 2014. Reservoir flood routing considering the non-stationarity of flood series in north China. *Water Resources Management* **28**(12): 4273–4287. DOI:10.1007/s11269-014-0744-6

Zhang Q, Gu X, Singh VP, Xiao M, Xu CY. 2014. Stationarity of annual flood peaks during 1951–2010 in the Pearl River Basin, China. *Journal of Hydrology* **519**Part D: 3263–3274. DOI:10.1016/j.jhydrol.2014.10.028

Zuo D, Xu Z, Wu W, Zhao J, Zhao F. 2014. Identification of streamflow response to climate change and human activities in the Wei River Basin, China. *Water Resources Management* **28**(3): 833–851. DOI:10.1007/s11269-014-0519-0